ASIA-PACIFIC METROLOGY PROGRAMME
500 MPa HYDRAULIC PRESSURE INTERLABORATORY COMPARISON
Comparison Identifier: **APMP.M.P-K13**

Final Report on Key Comparison APMP.M.P-K13 in Hydraulic Gauge Pressure from 50 MPa to 500 MPa

September 2014

Hiroaki Kajikawa[1], Tokihiko Kobata[1], Sanjay Yadav[2], Wu Jian[3], Tawat Changpan[4], Neville Owen[5], Li Yanhua[6], Chen-Chuan Hung[7], Gigin Ginanjar[8], In-Mook Choi[9]

[1]NMIJ/AIST (Pilot institute): National Metrology Institute of Japan, AIST, AIST Tsukuba Central 3, 1-1, Umezono 1-Chome, Tsukuba, Ibaraki, 305-8563 Japan

[2]NPLI: National Physical Laboratory, Dr. K. S. Krishnan Marg, New Delhi – 110 012, INDIA

[3]NMC/A*STAR: National Metrology Center, A*STAR, #02-27 National Metrology Centre, 1 Science Park Drive, Singapore 118221

[4]NIMT: National Institute of Metrology (Thailand), 3/4-5 Moo 3, Klong 5, Klong Luang, Pathumthani 12120 Thailand

[5]NMIA: National Measurement Institute Australia, Unit 1 – 153 Bertie Street Port Melbourne, Vic 3207 Australia

[6]NIM: National Institute of Metrology, China, Pressure and Vacuum Lab, NIM, Bei san huan dong lu 18, Beijing, China 100013

[7]CMS/ITRI: Center for Measurement Standards/ITRI, Room 109, Bldg. 08, 321 Kuang Fu Rd, Sec. 2, Hsinchu, Taiwan 300, R.O.C.

[8]KIM-LIPI: KIM-LIPI, Komplek Puspiptek Gedung 420 Cisauk-Tangerang, 15314 Indonesia

[9]KRISS: Korea Research Institute of Standards and Science, 1 Doryong, Yuseong, Daejeon, Rep. of Korea 305-340

Abstract

This report describes the results of a key comparison of hydraulic high-pressure standards at nine National Metrology Institutes (NMIs: NMIJ/AIST, NPLI, NMC/A*STAR, NIMT, NMIA, NIM, CMS/ITRI, KIM-LIPI, and KRISS) within the framework of the Asia-Pacific Metrology Programme (APMP) in order to determine their degrees of equivalence in the pressure range from 50 MPa to 500 MPa in gauge mode. The pilot institute was the National Metrology Institute of Japan (NMIJ/AIST). All participating institutes used hydraulic pressure balances as their pressure standards. A set of pressure balance with a free-deformational piston-cylinder assembly was used as the transfer standard. Three piston-cylinder assemblies, only one at a time, were used to complete the measurements in the period from November 2010 to January 2013. Ten participants completed their measurements and reported the pressure-dependent effective areas of the transfer standard at specified pressures with the associated uncertainties. Since one of the participants withdrew its results, the measurement results of the nine participants were finally compared. The results were linked to the CCM.P-K13 reference values through the results of two linking laboratories, NMIJ/AIST and NPLI. The degrees of equivalence were evaluated by the relative deviations of the participants' results from the CCM.P-K13 key comparison reference values, and their associated combined expanded (k=2) uncertainties. The results of all the nine participating NMIs agree with the CCM.P-K13 reference values within their expanded (k=2) uncertainties in the entire pressure range from 50 MPa to 500 MPa.

Contents

1. Introduction

The National Metrology Institute of Japan (NMIJ/AIST), Japan, has been agreed by the Technical Committee for Mass and Related Quantities (TCM) in the Asia-Pacific Metrology Programme (APMP) to coordinate an interlaboratory comparison program for high-pressure as a pilot institute. The comparison was identified as **APMP.M.P-K13** by the Consultative Committee for Mass and Related Quantities (CCM) of the International Committee for Weights and Measures (CIPM), the International Bureau of Weights and Measures (BIPM) and APMP. The objective of the comparison was to compare the performance of hydraulic pressure standards in the National Metrology Institutes (NMIs), in the pressure range 50 MPa to 500 MPa for gauge mode according to the guidelines[1,2,3]. To gain an international acceptance for the pressure standards, the results of APMP.M.P-K13 will be linked to the CCM key comparison, CCM.P-K13[4], which was conducted at the same pressure range as APMP.M.P-K13. All participating institutes have the opportunity to get results in the comparison at a level of uncertainty appropriate for them[5]. The results of this comparison will be included in the Key Comparison Database (KCDB) of BIPM following the rules of CCM and will be used to establish the degree of equivalence of national measurement standard by NMIs[6]. Those are essential supporting evidence for high-pressure calibration and measurement capabilities (CMCs) of NMIs for the Mutual Recognition Arrangement (MRA)[1].

The pilot institute, NMIJ/AIST, sent an invitation to APMP TCM members of on June 2010, and then, 13 institutes, including the pilot institute, announced their participation to this comparison. A protocol was prepared by the pilot institute, which was approved by the participants in December 2010 with some modifications. The protocol was revised several times during the whole period of comparison due to the change in piston-cylinder assembly circulated and measurement schedule. In this comparison, a set of pressure balance utilizing three piston cylinder assemblies was used as the transfer standard. After the characterizations and initial measurements at the pilot institute, the three piston-cylinder assemblies of the transfer standard, only one at a time, were circulated to participants from November 2010 to January 2013 as per agreed time schedule. All the NMIs used hydraulic pressure balances as their pressure standards and calibrated the transfer standard against the standard pressure balance following the protocol[7]. Although initially 13 institutes agreed to perform measurements, ten participants finally completed the measurements and submitted the reports to the pilot institute by April 2013. The participants reported the effective area of the piston-cylinder circulated, and the associated uncertainties. The pilot institute analyzed the reported data

from the participants and prepared a report of the comparison according to the guidelines[1,2,3].

This report describes the comparison results of the transfer standard carried out at nine NMIs, since one of the participants decided to withdraw from the comparison after a draft report was circulated. The following sections provide descriptions of the participants and their pressure standards, the transfer standard, the circulation of the transfer standard, the general measurement procedure for the transfer standard, the method for analysis of the calibration data, results of the participants, and linking to the CCM.P-K13.

2. Participating institutes and their pressure standards

2.1 List of participating institutes

Nine NMIs finally participated in this comparison including the pilot institute. The participating institutes along with their addresses for contacts are listed in Table 2.1 in the order of their performing measurements. The index number (ID) in the first column is used to identify the participating institute in this report. Other three institutes also participated in this comparison. SIRIM (Malaysia) and NIS (Egypt) withdrew from the comparison due to breakage of the piston-cylinder of the transfer standard. KazInMetr (Kazakhstan), which does not have any pressure CMCs, completed their measurements and submitted a report, but decided to withdraw from the comparison after the draft B report was circulated. Therefore, these three institutes are not included in the list.

Table 2.1: List of the participating institutes.

ID	Participating institutes	Contact Persons
1	**Country:** Japan **Acronym:** NMIJ/AIST (Pilot institute) **Institute:** National Metrology Institute of Japan, AIST **Address:** AIST Tsukuba Central 3, 1-1, Umezono 1-Chome, Tsukuba, Ibaraki, 305-8563 Japan	**Name:** Dr. Tokihiko Kobata, Dr. Hiroaki Kajikawa **Tel:** +81-298-61-4378 **Fax:** +81-298-61-4379 **E-mail:** tokihiko.kobata@aist.go.jp, kajikawa.hiroaki@aist.go.jp
2	**Country:** India **Acronym:** NPLI **Institute:** National Physical Laboratory **Address:** Vacuum and Pressure Standards National Physical laboratory Dr. K. S. Krishnan Marg New Delhi – 110 012, INDIA	**Name:** Dr. A. K. Bandyopadhyay, Dr. Sanjay Yadav **Tel:** 91-11-45608593 **Fax:** 91-11-45609310 **E-mail:** akband@mail.nplindia.org, syadav@mail.nplindia.org
3	**Country:** Singapore **Acronym:** NMC/A*STAR **Institute:** NMC/A*STAR **Address:**	**Name:** Mr. Wu Jian **Tel:** 65-6279 1961 (O) **Fax:** 65-6279 1993 **E-mail:** wu_jian@nmc.a-star.edu.sg

	#02-27 National Metrology Centre, 1 Science Park Drive, Singapore 118221	
4	**Country:** Thailand **Acronym:** NIMT **Institute:** National Institute of Metrology (Thailand) **Address:** 3/4-5 Moo 3, Klong 5, Klong Luang, Pathumthani 12120 Thailand	**Name:** Mr. Tawat Changpan **Tel:** +66 2577 5100 extension 1230 **Fax:** +66 2577 3658 **E-mail:** tawat@nimt.or.th
5	**Country:** Australia **Acronym:** NMIA **Institute:** National Measurement Institute Australia **Address:** Unit 1 – 153 Bertie Street Port Melbourne, Vic 3207 Australia	**Name:** Mr. Neville Owen Mr. Kevin Mapson **Tel:** 03 9644 4907 **Fax:** 03 9644 4900 **E-mail:** Neville.owen@measurement.gov.au kevin.mapson@measurement.gov.au
6	**Country:** China **Acronym:** NIM **Institute:** National Institute of Metrology, China **Address:** Pressure and Vacuum Lab, NIM, Bei san huan dong lu 18, Beijing, China 100013	**Name:** Ms. Li Yanhua **Tel:** +86-10-64525115 **Fax:** +86-10-64218637 **E-mail:** liyh@nim.ac.cn
7	**Country:** Chinese Taipei **Acronym:** CMS/ITRI **Institute:** Center for Measurement Standards / ITRI **Address:** Room 109, Bldg. 08, 321 Kuang Fu Rd, Sec. 2, Hsinchu, Taiwan 300, R.O.C.	**Name:** Mr. Chen-Chuan Hung **Tel:** 886-3-5743788 **Fax:** 886-3-5724952 **E-mail:** c-chung@itri.org.tw

8	**Country:** Indonesia **Acronym:** KIM-LIPI **Institute:** KIM-LIPI **Address:** Komplek Puspiptek Gedung 420 Cisauk-Tangerang, 15314 Indonesia	**Name:** Ms.Renanta Hayu, Mr.Gigin Ginanjar **Tel:** +62 21 7560562 ext 3086 **Fax:** +62 21 7560064 **E-mail:** renanta@kim.lipi.go.id, gigin@kim.lipi.go.id
9	**Country:** Republic of Korea **Acronym:** KRISS **Institute:** Korea Research Institute of Standards and Science **Address:** 1 Doryong, Yuseong, Daejeon, Rep. of Korea 305-340	**Name:** Dr. In-Mook Choi, Dr. Sam-Yong Woo **Tel:** +82-42-868-5118 **Fax:** +82-42-868-5022 **E-mail:** mookin@kriss.re.kr, sywoo@kriss.re.kr

2.2 Pressure standards of participating institutes

All the participating institutes used pressure balances of different manufacture and model as their laboratory standards. Pressure balances were equipped with a simple type or a re-entrant type piston-cylinder assembly. Each participating institute provided information about their standard that was used to calibrate the transfer standard to the pilot institute. Table 2.2 lists the information about the laboratory standards, including the pressure balance base, the type and material for piston-cylinder assembly, the effective area with associated standard uncertainty, the reference temperature, the pressure distortion coefficient with associated standard uncertainty, and the method and rotation rate of the piston. Most of the participating institutes assumed linear pressure dependence for the effective area of piston-cylinder assembly, except for NMIJ/AIST which uses a quadratic function of pressure. The participating institutes which independently establish the primary standards from base SI units were NMIJ/AIST, NPLI, NMIA, NIM and KRISS.

Table 2.2: Summary of laboratory standards of the participating institutes.

i	Institute	Traceability	Pressure balance base		Piston-cylinder		Rotation	
			Manufacturer	Model	Type	Material	Method	[rpm]
1	NMIJ/AIST	Independent	DH Instruments, Fluke	7302	Simple	WC/WC	Hand	20 - 30
2	NPLI	Independent	DH-budenberg	5306	Simple	Steel/WC	Motor	20 - 30
3	NMC/A*STAR	PTB	Ruska	2485	Simple	WC/WC	Hand	20 - 30
4	NIMT	NMIJ	DH Instruments, Fluke	7302	Simple	WC/WC	Motor	25
5	NMIA	Independent	DH Instruments, Fluke	7302	Simple	WC/WC	Hand	20 - 30
6	NIM	Indipendent	DH Instruments, Fluke	7302	Simple	WC/WC	Motor	19 - 22
7	CMS/ITRI	PTB	Ruska	2450-700	Reentrant	WC/WC	Hand	22 - 24
8	KIM-LIPI	NMIJ	DH Instruments, Fluke	7302	Simple	WC/WC	Motor	20
9	KRISS	Independent	DH Instruments, Fluke, DH	7302, 5306	Simple	WC/WC	Hand	10 - 20

Table 2.3: Effective area and pressure distortion coefficient of laboratory standards. All the uncertainties are expressed as the standard ones.

i	Institute	Effective area A_{tr}			Ref. temp	Distortion coefficient λ_1 [MPa^{-1}]		Distortion coefficient λ_2 [MPa^{-2}]	
		Value [m^2]	Unc. [m^2]	Unc. [ppm]	t_r [°C]	Value [MPa^{-1}]	Unc.[MPa^{-1}]	Value [MPa^{-2}]	Unc.[MPa^{-2}]
1	NMIJ/AIST	1.960899E-06		15.5	23	7.53E-07	5.60E-08	5.80E-11	6.50E-11
2	NPLI	1.960786E-06		9.2	20	8.23E-07	8.25E-09		
3	NMC/A*STAR	2.373090E-06	5.50E-11	23.2	20	7.0E-07	2.8E-07		
4	NIMT	1.961378E-06			20	8.45E-07	1.30E-07		
5	NMIA	1.960193E-06	2.1E-11	10.7	20	9.9E-07	7.5E-08		
6	NIM	1.962256E-06		19.1	20	8.58E-07	8.3E-08		
7	CMS/ITRI	8.40231E-06	2.0E-10	23.8	20	-2.7E-06	1.0E-07		
8	KIM-LIPI	1.961203E-06	2.9E-11	14.8	20	8.5E-07	8.4E-08		
9	KRISS	1.961063E-06	3.5E-11	17.8	23	7.80E-07	7.0E-08		

2.3 Details of traceability of pressure standards

In addition to the basic information listed above, participating institutes also provided details about method of establishing their pressure standard, as described herein;

2.3.1 NMIJ

The effective area of the laboratory standard (LS) was determined by cross-float measurements with several piston-cylinders: free-deformation (FD) piston-cylinder (1 MPa/kg up to 100 MPa) and NMIJ/AIST controlled-clearance (CC) piston-cylinders (0.2 MPa/kg and 0.5 MPa/kg up to 200 MPa and 500 MPa, respectively). The FD piston-cylinder of 1 MPa/kg was used for CCM. P-K7, and is traceable through a series of calibrations to larger piston-cylinder assemblies whose effective areas have been evaluated by the NMIJ/AIST mercury manometer and/or dimensional measurements. The large pressure balance using CC piston-cylinders have been originally developed in cooperation with Nagano Keiki Co., Ltd[8]. The pressure dependence of the effective area of the CC piston-cylinders has been estimated experimentally based on the Heydemann-Welch model[9].

From the cross-float measurements, the effective area of the LS over the whole pressure range is expressed by a quadratic function of pressure: $A = A_0 * (1 + \lambda_1 * p + \lambda_2 * p_2)$. The parameters are listed in Table 2.3. The uncertainties of the parameters, $u(A_0)$, $u(\lambda_1)$, $u(\lambda_2)$, are determined so that the relative combined uncertainty of the effective area from the cross-float measurements, u(A), are approximated by the equation: $u^2(A) = (u(A_0)/A_0)^2 + (u(\lambda_1) * p)^2 + (u(\lambda_2) * p^2)^2$.

Uncertainty of the pressure dependence of the effective area is estimated from the uncertainty of the parameters in the Heydemann-Welch model, zero clearance jacket pressure and jacket pressure coefficient, and of other influential factors in the characterization experiments[10].

2.3.2 NPLI

The laboratory standard (LS), designated as NPL500MPN, used in the comparison is a simple design type piston gauge having working pressure range of (1 – 500) MPa. The laboratory standard determines the pressure through A_0 and λ, which are obtained by calibrating LS against controlled clearance type primary hydraulic pressure standard. The traceability of primary standard is achieved through mass calibration against national standards of mass and balances and dimensional measurements against national standards of length and dimension. Thus, the LS is traceable to national primary pressure standard through unbroken chain of national standards of mass, length and pressure.

2.3.3 NMC/A*STAR

The zero-pressure effective area and the pressure distortion coefficient were calculated from PTB certificate no. 0011PTB08.

2.3.4 NIMT

The zero-pressure effective area and the pressure distortion coefficient were calculated by NIMT by using standard pressure from NMIJ certificate no. 073145.

2.3.5 NMIA

NMIA has established a primary 10 MPa reference piston gauge by dimensional measurement and finite element analysis modelling of a nominal 490 mm^2 tungsten carbide (piston and cylinder) piston gauge. This piston gauge provides traceability for A_0, and is one of the three harmonised sources for the traceability in λ_1. This piston gauge has a declared A_0 value of 490.258 9 mm^2 with a standard uncertainty (k=1) of 0.003 65 mm^2. The λ_1 value for this piston gauge is 1.12×10^{-6} MPa^{-1} with a standard uncertainty (k=1) of 0.085×10^{-6} MPa^{-1}. The A_0 value for the NMIA 500 MPa piston gauge used in the APMP.M.P-K13 comparison is traced to the nominal 490 mm^2 primary piston gauge by cross float calibration of a set of simple free deformation piston gauges.

The λ_1 value for the NMIA 500 MPa piston gauge is traced to the nominal 490 mm^2 primary piston gauge, LNE and a NMIA controlled clearance piston gauge. The λ_1 value for the NMIA 500 MPa piston gauge is established by cross float calibration of a set of simple free deformation piston gauges. The variation associated with the pressure distortion disseminated from these three sources has been included in the uncertainty of the λ_1 value for NMIA 500 MPa piston gauge.

The source uncertainties (k=1) for λ_1 are 8.5×10^{-8} MPa^{-1} for the NMIA dimensionally measured and modelled piston gauge, and 2.8×10^{-8} MPa^{-1} for the LNE calibration of the NMIA 100 MPa piston gauge. The cross float calibration, combination and harmonization process results in a working λ_1 uncertainty of 5.5×10^{-8} MPa^{-1} for the NMIA 100 MPa piston gauge and 7.5×10^{-8} MPa^{-1} for the NMIA 500 MPa piston gauge.

2.3.6 NIM

The NIM national pressure standard participated in the KC was a free-deformation (FD) piston-cylinder manufactured by DHI, whose effective area was determined by the cross-float measurements with a 2 MPa/kg controlled-clearance (CC) piston-cylinder up to 200 MPa. The CC piston-cylinder is also a DHI product and the

piston area was traced through a series of calibrations to the NIM primary pressure standards in the range of 10 MPa. The NIM primary pressure standards are a group of five piston-cylinders with nominal effective areas of 1 cm^2 and maximum load of 100 kg, whose effective areas were determined by the dimensional measurements and inter-comparisons[11]. The pressure dependence of the effective area of the CC piston-cylinder was evaluated using the Heydemann-Welch method[9].

The A_0 and λ of the LS were determined by the linear fitting of the effective area obtained from the cross-float measurements from the expression: $A_p=A_0(1+\lambda_p)$. The uncertainty of λ is a combination of the standard deviation and the uncertainty originated from the pressure dependence of the effective area of the CC piston-cylinder. The uncertainty of A_0 is then estimated from the uncertainty of the piston area of the CC piston-cylinder and the standard deviation.

2.3.7 CMS/ITRI

The effective area $A_{0,}$ $\lambda_{1,}$ and the weight of total mass were traceable to PTB in 2011.

2.3.8 KIM-LIPI

The pressure balance is traceable to NMIJ (certificate number: 092005) that issued in January 26th 2009. Value and uncertainty for A_0 and λ_1 were calculated using linear regression fit which is based on NMIJ certificate above.

2.3.9 KRISS

The zero-pressure effective area (A_0) of the 500 MPa pressure standard has been determined by cross-float measurements with several piston-cylinder units, which are 1.0 MPa/kg up to 100 MPa, 2.0 MPa/kg up to 200 MPa in FD mode, 2.0 MPa/kg up to 500 MPa in CC mode. 1.0 MPa/kg piston-cylinder unit was used for the key comparison of APMP.M.P-K7, which is traceable to dimensional measurements of 10 kPa/kg piston-cylinder unit. The value of the distortion coefficient (λ) with associated uncertainty was determined by FEA and an experimental method.

1 GPa pressure standard uses a piston-cylinder unit (2 MPa/kg) with 500 kg deadweight and can be operated in CC mode. The distortion coefficients have been determined by FEA in FD and CC modes.

From the cross-float measurements, the effective area of the 500 MPa pressure standard over the whole pressure range is expressed by a function of pressure: $A_p=A_0(1+\lambda*p)$.

3. Transfer standard

3.1 Components of transfer standard

A pressure balance with a piston-cylinder with 1.96 mm^2 of the nominal effective area was used as the transfer standard (TS). In this comparison, one of three piston-cylinder assemblies, identified by serial number 1510 (Petal 1), 1562 (Petal 2 and 3) or 1648 (Petal 4), was circulated. All the parts of the pressure balance, including an instrument platform PG7302, PG terminal, a mass loading bell, were manufactured by Fluke Calibration, USA. The set of the pressure balance was borrowed from Fluke Calibration, and returned back to them after completing all of the measurements.

All the parts of the pressure balance, except an optional mass set, were packed into a single carrying box. An electric device for measuring environmental condition (Model TR-73U) and three gravity shock recorders (G-MEN DR10) were included in the box for measuring the condition during transportation. The measuring data were saved into the internal memory of the device and extracted at the pilot institute using a special device and software. Accessories, cables for the pressure balance, reserve parts, copies of the manual and the protocol for this comparison were also packed in the same box. The components of the transfer package are listed in Table 3.1. The total weight of the package was approximately 33 kg. The total cost declared for the transfer standard was 5,400,100 JPY. Components of the transfer standard are shown in Fig. 3.1, and the packing of the transfer standard is illustrated in Fig. 3.2. An optional mass set was sent to participants not having weights for PG7302. The mass set was separately packed into four carrying boxes, as listed in Table 3.2.

Table 3.1: Components of transfer standard.

1.	Piston-cylinder assembly PC-7300-5 in carrying case (1) SN 1510 (Petal 1), SN 1562 (Petal 2 and 3), or SN 1648 (Petal 4)
2.	Instrument platform PG7302, SN 809 (1) 360 mm H x 400 mm W x 350 mm D, 13 kg
3.	PG terminal PG7000 (1) 120 mm H x 150 mm W x 200 mm D, 1.4 kg
4.	Mass loading bell PG7000, SN 926 (1)
5.	Temperature probe, SN U808 (built in pressure balance) (1)
6.	Oil run-off pan (built in pressure balance) (1)
7.	Connecting cable for PG terminal (1)
8.	Power supply cord (1)
9.	Plug for connecting port (1)
10.	Orange-colored cap for mounting post (1)
11.	PG7000™ PISTON GAUGES PG7102™, PG7202™, PG7302™, PG7601™ (Ver. 3.0 and Higher) Operation and Maintenance Manual[12] (1)
12.	Protocol[7](1)
13.	Environment measuring device (Model TR-73U) (1)
14.	Gravity shock recorder (G-MEN DR10) (3)
15.	O-rings for PC-7300-5 [Reserve parts] (L: 5, S: 1)
16.	Collar for DH500 [Reserve parts] (1)
17.	Gland nut for DH500 [Reserve parts] (1)
18.	Molded transit case with foam inserts (1) 530 mm D x 650 mm W x 480 mm H

Table 3.2: Components of optional mass set.

1.	Mass set PG7000 MS-7002-100, SN 2637 (1 kg: 1, 2 kg: 2, 5 kg: 1, 9 kg: 1, 10 kg: 8)
2	Molded transit cases with foam inserts (4)

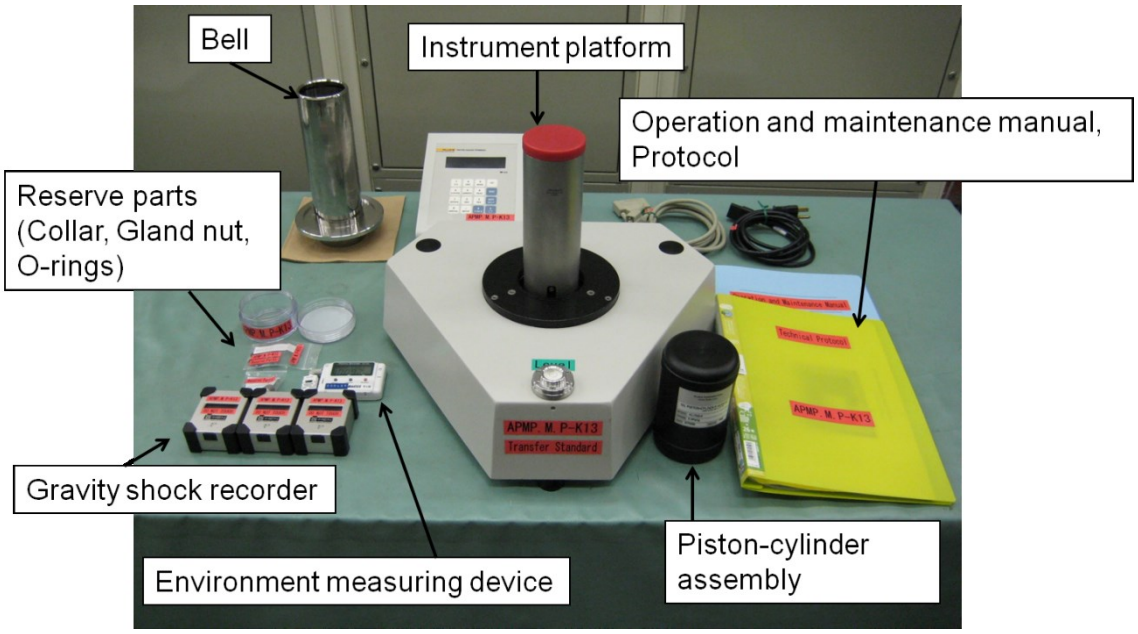

Figure 3.1: Components of transfer standard for APMP.M.P-K13.

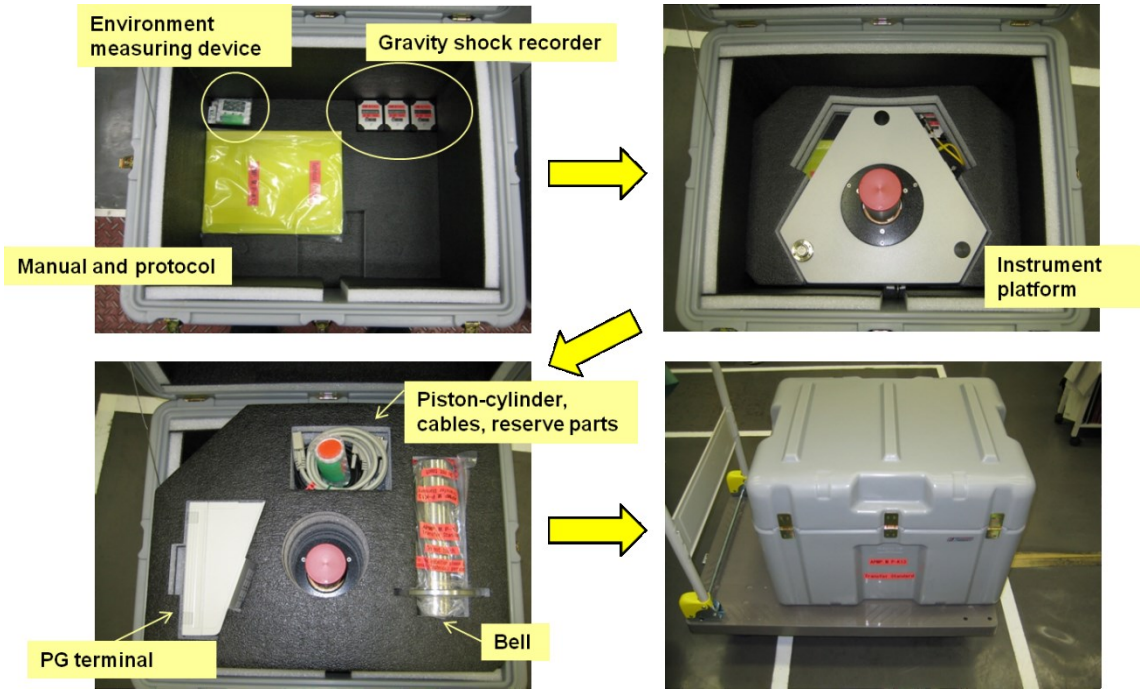

Figure 3.2: Packing of transfer standard.

3.2 Characteristics of transfer standard

3.2.1 Piston-cylinder assembly:

Each of the piston-cylinder assembly used in TS for this comparison is of simple type. The nominal effective area of the assembly $A'_{0,nom}$ is 1.96 mm^2. The measurement range is up to 500 MPa with a total of 100 kg of weights. Both piston and cylinder of the TS are made of tungsten carbide with the following linear thermal expansion coefficient (α), Young's modulus (E) and Poisson's coefficient (μ) [13], as listed in Table 3.3.

Table 3.3: Characteristics of piston-cylinder assembly.

	Material	α [°C^{-1}]	E [GPa]	μ
Piston	Tungsten carbide	$4.5 \cdot 10^{-6}$	560	0.218
Cylinder	Tungsten carbide	$4.5 \cdot 10^{-6}$	620	0.218

The thermal expansion coefficient of the piston-cylinder unit can be taken as $\alpha'_p + \alpha'_c = (9.00 \pm 0.22) \cdot 10^{-6}$ °C^{-1}.

The piston head is made of titanium. The piston cap and the screw and adjusting mass are made of 304 L stainless steel. The value of equivalent density was provided by the manufacturer[13], as listed in Table 3.4. The true mass and length (distance from the piston lower face to the upper piston cup edge) of the piston is measured at the pilot institute as in Table 3.4, which were provided to the participants.

Table 3.4: Mass, density and length of the pistons.

	True mass [g]	Equivalent density [kg/m^3]	Piston length [mm]
SN 1510	200.0017 ± 0.0010	$7320 \cdot (1 \pm 1 \cdot 10^{-2})$	90.11 ± 0.01
SN 1562	200.0017 ± 0.0010	$7320 \cdot (1 \pm 1 \cdot 10^{-2})$	90.19 ± 0.01
SN 1648	200.0009 ± 0.0010	$7320 \cdot (1 \pm 1 \cdot 10^{-2})$	90.01 ± 0.01

The magnetization of the piston and cylinder was checked so that the magnetic flux density at their surfaces was not higher than 2 x 10^{-4} Tesla.

3.2.2 Reference level and piston working position:

The reference level of the TS is indicated on the mounting post of the platform. The recommended piston working position is physically about (4.3 ± 0.5) mm above its lowermost (low-stop) position. When the piston works in the recommended position range, the bottom of the piston gives close agreement with the reference level of the TS. The pilot institute confirmed that there is no systematic change in the effective area for

the piston positions of (4.3 ± 1.0) mm above its low-stop position.

3.2.3 Typical cross-float sensitivity and reproducibility:

The relative cross-float sensitivity is better than $2 \cdot 10^{-6}$ in the pressure range from 50 MPa to 500 MPa.

The relative experimental standard deviations of single values of the effective areas at the measurement pressures lie typically between (1 and 3)$\cdot 10^{-6}$.

3.2.4 Piston fall rates:

Piston fall rates (v_f) were measured by the pilot institute at temperatures around 23 °C, as listed in Table 3.5.

Table 3.5: Piston fall rates of the pistons.

p [MPa]	v_f [mm/min] (SN 1510)	v_f [mm/min] (SN 1562)	v_f [mm/min] (SN 1648)
50	0.08	0.03	0.03
100	0.18	0.07	0.08
150	0.26	0.12	0.11
200	0.33	0.16	0.14
250	0.38	0.18	0.18
300	0.37	0.20	0.22
350	0.38	0.21	0.22
400	0.39	0.22	0.24
450	0.40	0.23	0.25
500	0.42	0.27	0.25

3.2.5 Piston free rotation time:

When piston rotates freely (without motor) at a pressure of 50 MPa and a temperature of 23 °C, the rotation speed descends

from 30 rpm to 22 rpm within 30 minutes (SN 1510),

from 30 rpm to 25 rpm within 20 minutes (SN 1562),

from 30 rpm to 22 rpm within 30 minutes (SN 1648).

3.2.6 Mass loading bell, mass and density:

The mass loading bell, serial number 926, is made of composite of 6AL-4V titanium, low carbon steel with nickel plate and AISI 304L non-magnetic stainless steel. True mass and the equivalent density are listed in Table 3.6.

Table 3.6: Mass and density of the mass loading bell.

	True mass [g]	Equivalent density [kg/m^3] [13]
Mass loading bell	800.0014 ± 0.0010	$6058 \cdot (1 \pm 1 \cdot 10^{-2})$

3.2.7 Temperature probe:

The temperature of the piston-cylinder assembly (*t'*) is measured with a platinum resistance thermometer (PRT) housed in the mounting post of PG7302, and is displayed on the PG terminal. At the pilot institute, the platinum resistance thermometer (PRT) was calibrated with the standard uncertainty of 0.02 °C in the temperature range (20.0 to 26.0) °C. From the calibration, the following parameters are entered in the PG terminal: RZ = 100.02, S = 0.3877.

4. Circulation of transfer standard

4.1 Chronology of measurements

According to the protocol[7], the transfer package was circulated during the period from November 2010 to January 2013. The comparison was organized on a petal basis with the transfer packages returning periodically to the pilot institute (NMIJ/AIST) for check and calibration. The participants were divided into four groups (Petal 1 to Petal 4). The allotted time period for measurement at each participant was 26 days (3 weeks and 5 days), and two weeks were allotted for the transportation of the transfer standard. However, the measurement schedule was changed from the initial plan because of delays in custom clearance procedures and also damage of the transfer standard. The piston-cylinder asssmbly of SN 1510 was broken in pieces during the measurements at NML-SIRIM in Petal 1. The transfer standard was once returned back to the pilot institute, and circulated to the next participant with a new piston-cylinder assembly SN 1562. The SN 1562 was also broken during the installation at NIS in Petal 3. Then, the measurements in Petal 4 were conducted with the third piston-cylinder SN 1648.

The actual arrival and departure dates of the transfer standard, and the measurement dates for three cycles are listed in Table 4.1. These dates were taken from arrival and departure reports, Appendix A1 and A2 in the protocol, and individual results sheets, Appendix A6 in the protocol, which were submitted from the participants to the pilot institute. The results of the three participants in grey-colored columns are not included in the report because of measurement cancellation or withdrawal.

Table 4.1: Chronology of measurements.

Petal	PC	Institute	Arrival	Measurements	Departure
1	1510	NMIJ/AIST	---	Nov. 15-18, 2010 Dec. 3-8, 2010	Dec. 15, 2010
		NPLI	Dec. 31, 2010	Jan. 14-16, 2011	Feb. 4, 2011
		NML/SIRIM	Mar. 9, 2011	---	---
2	1562	NMIJ/AIST	---	May 12-16, 2011	Jun. 2, 2011
		NMC/A*STAR	Jun. 14, 2011	Jun. 27-29, 2011	Jul. 8, 2011
		NIMT	Jul. 29, 2011	Aug. 11-13, 2011	Aug. 19, 2011
		NMIA	Aug. 29, 2011	Sep. 20-27, 2011	Sep. 29, 2011
3		NMIJ/AIST	Oct. 14, 2011	Oct. 24-27, 2011	Nov. 21, 2011
		NIM	Dec. 9, 2011	Dec. 21-23, 2011	Jan. 5, 2012
		CMS/ITRI	Jan. 12, 2012	Feb. 3-7, 2012	Feb. 15, 2012
		NIS	Mar. 12, 2012	---	---
4	1648	NMIJ/AIST	---	May 18-22, 2012	Jun. 26, 2012
		KIM-LIPI	Jul. 14, 2012	Aug. 1-3, 2012	Sep. 4, 2012
		KazInMetr	Sep. 9, 2012	Oct. 8-12, 2012	Oct. 24, 2012
		KRISS	Nov. 9, 2012	Nov. 20-22, 2012	Dec. 10, 2012
		NMIJ/AIST	Dec. 19, 2012	Jan. 10-15, 2013	---

4.2 Environmental conditions during comparisons

Three gravity shock recorders and an environment monitoring device were included in the transfer standard to check the conditions during transportations, as listed in Table 3.1. The environment monitoring device measures temperature, atmospheric pressure, and relative humidity. The gravity shock recorder measures acceleration along three axes. The obtained data were saved in their memories during a loop and extracted by the pilot institute after each loop.

Environmental conditions during transportations and measurements were shown in Fig. 4.1 for Petal 1, Fig. 4.2 for Petal 2, Fig. 4.3 for Petal 3, and Fig. 4.4 for Petal 4. In each figure, figure (a) shows the acceleration; the data for three axes are composed to produce the absolute value of a total impact. From the acceleration data, we can see when the transfer standard is moved and when an impact is applied to the transfer standard. A large impact was found to be applied mainly at airports before and after the air-freight. Figure (b) shows the temperature. The transfer standard is sometimes placed at very high temperature around 35 ^{o}C, or below 5 ^{o}C during transportations. From the atmospheric pressure in figure (c), we can see when the transfer standard is carried by air-freight. The humidity, shown in figure (d) sometimes changes rapidly with temperature change during transportation, then ranges from 10 % to 90 %. It should be noted that these devices were always installed in the transit case, and then did not necessarily show the environmental conditions during measurements at each laboratory. These data were used only for checking the conditions and treatments during transportations.

In some places, temperature and humidity exceeds the normal permissible ranges, and relatively large impacts were recorded during transportations, mainly at airports. However, any severe damages were not reported from the participants, except for the blemish and markings probably made by custom personnel, and breakage of a small clip on the pressure balance base.

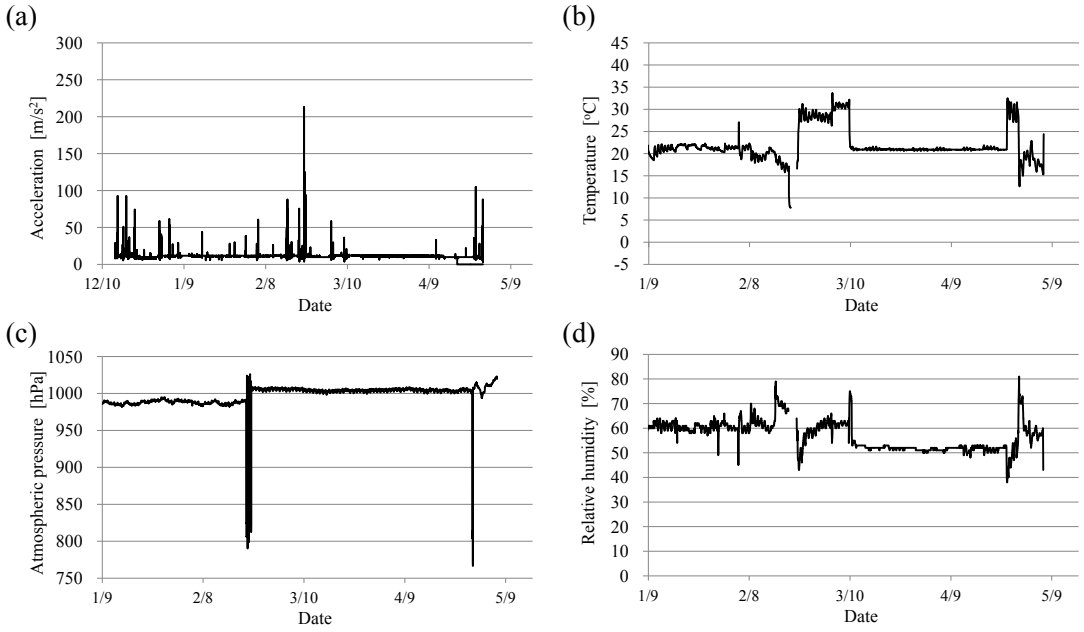

Figure 4.1: Environmental conditions during Petal 1.

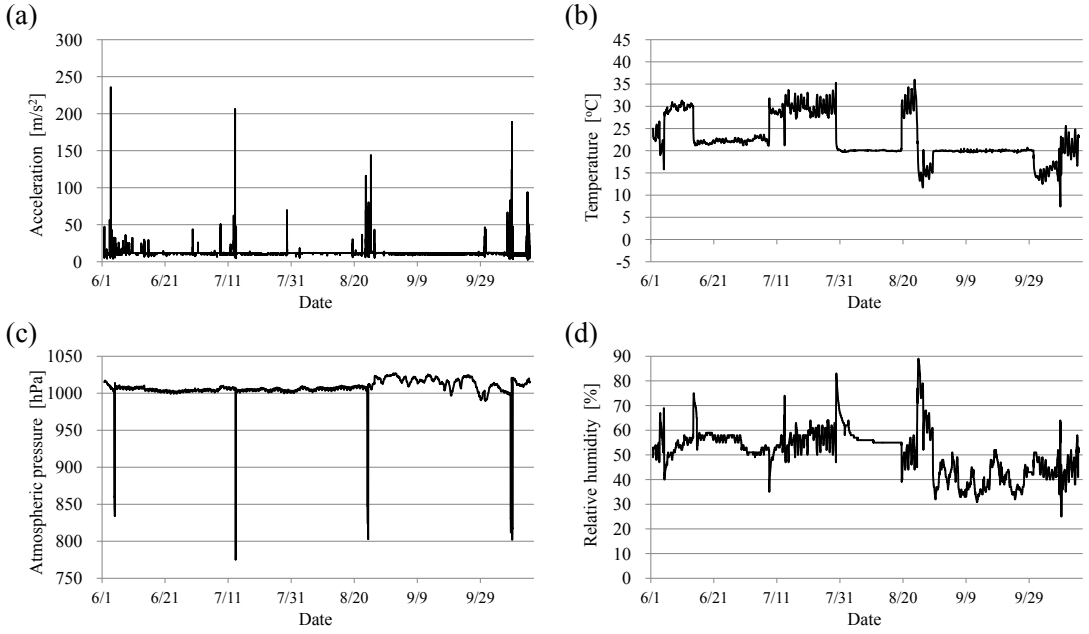

Figure 4.2: Environmental conditions during Petal 2.

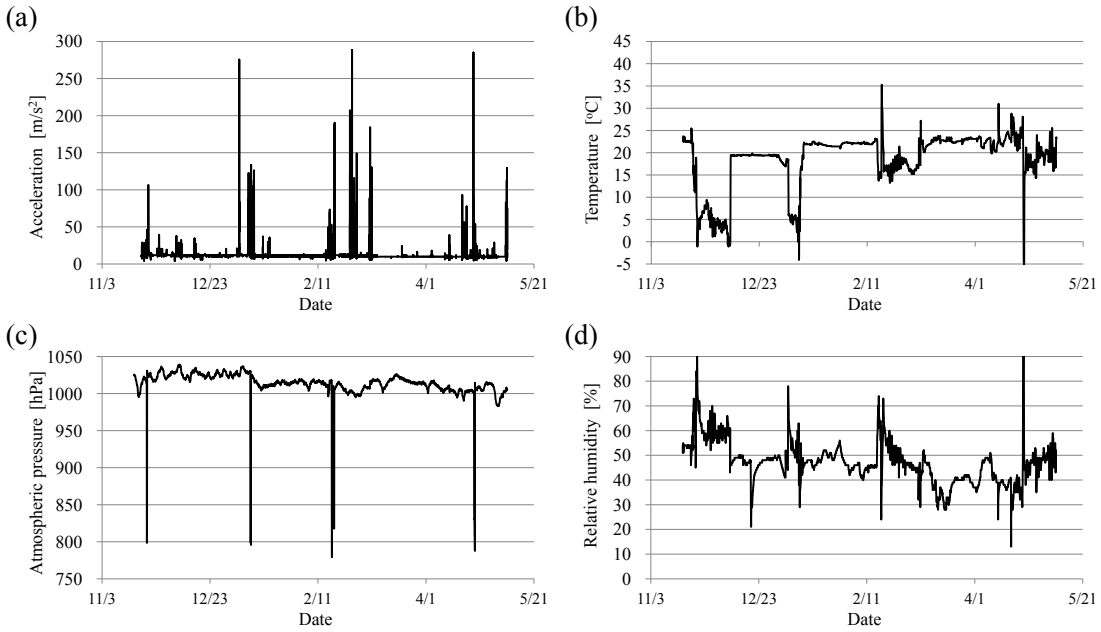

Figure 4.3: Environmental conditions during Petal 3.

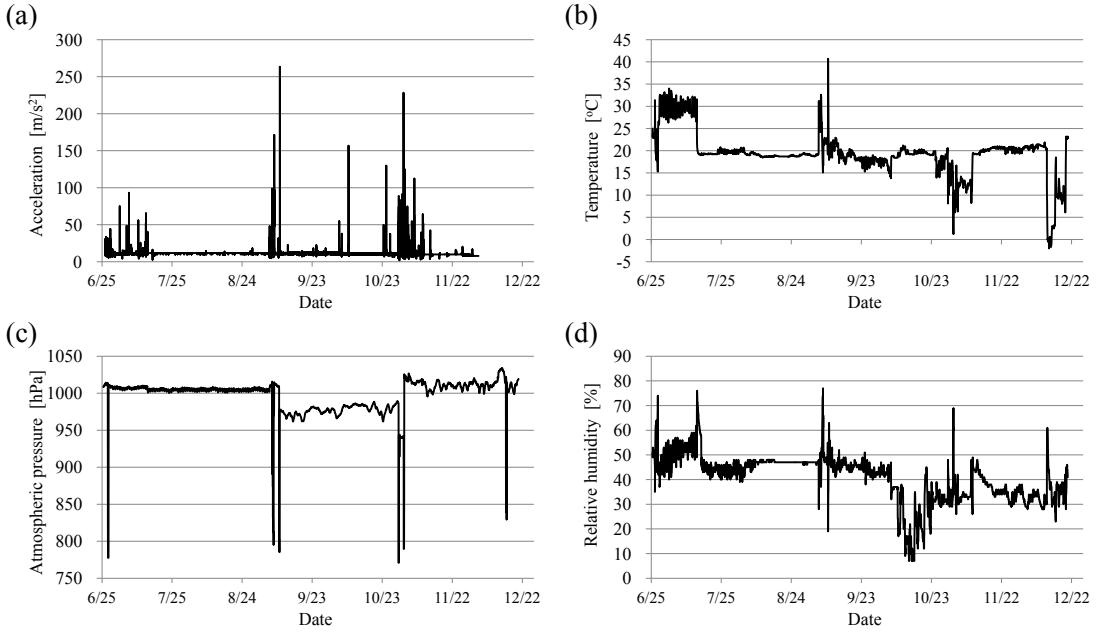

Figure 4.4: Environmental conditions during Petal 4.

5. Measurement

The general measurement procedure and instructions for operating the TS are described in the protocol[7]and Operation and Maintenance Manual[12], which were sent to the participants.

5.1 Measurement conditions and preparation

Clean Dioctyl sebacate (DOS) was required to be used as a pressure transmitting medium. Participants prepared DOS by themselves. The properties of DOS, density and surface tension, were provided in the protocol[7] by the pilot institute as follows:

$$\rho_{DOS} = [912.7 + 0.752(p/\text{MPa}) - 1.65\cdot10^{-3}(p/\text{MPa})^2 + 1.5\cdot10^{-6}\,(p/\text{MPa})^3] \times [1 - 7.8\cdot10^{-4}\,(t/°\text{C} - 20)] \times (1 \pm 0.01)\ [\text{kg/m}^3]\ .$$

The surface tension (σ) of DOS is $\sigma = 31.2$ x (1 ± 0.05) [mN/m].

TS was powered on at least 12 hours before starting the measurement, for warming up and stabilization.

The piston-cylinder assembly was mounted in the platform carefully in accordance with the instructions given in the Operation and Maintenance Manual[12]. The verticality of the piston and cylinder was adjusted in the participant's manner.

After the installation, TS was pressurized up to 500 MPa, and the leak in the calibration system was checked. To check the tightness of TS, the piston fall rate was measured preferably at pressures of (500, 250 and 50) MPa. It was required to wait a minimum of 10 minutes after generating the pressure in the TS measurement system prior to starting the piston fall rate measurements in order to stabilize the TS temperature. The typical piston fall rate was provided by the pilot institute.

The reference temperature of the comparison is 20 °C. If measurements were performed at a temperature deviating from 20 °C, the effective area of TS was referred to 20 °C using the piston-cylinder thermal expansion coefficient given in the protocol.

5.2 Measurement procedures

The measurements include three cycles each with nominal pressures generated in the following order (50, 100, 150, 200, 250, 300 350, 400, 450, 500, 500, 450, 400, 350, 300, 250, 200, 150, 100, 50) MPa. The generated pressures at the reference level of the TS were controlled not to deviate from these nominal values by more than 0.1 MPa. Totally 60 measurements were conducted. The time between a pressure level change and the acquisition of the data corresponding to the equilibrium of the participant's standard

and TS was not shorter than 5 minutes. The time between two consequent measurements at 500 MPa was at least 15 minutes. One complete measurement cycle was performed in one day. Measurements were repeated two more times with each cycle being on a separate day.

The piston working position was measured using the participant's own devices. The recommended piston working position was physically about (4.3 ± 0.5) mm above its low-stop position. The recommended rotation speed is between 20 and 30 rpm.

5.3 Reporting of the results

Each participant reported the effective area of TS piston-cylinder at each measurement pressure (A'_{p}). The pressure generated by a pressure standard at the reference level of the TS, p', is represented by the following equation:

$$p' = p_{\mathrm{s}} + (\rho_{\mathrm{f}} - \rho_{\mathrm{a}}) \cdot g \cdot h \,, \qquad (5.1)$$

where p_{s} is the pressure generated by the participant's pressure standard at its reference level; $(\rho_{\mathrm{f}} - \rho_{\mathrm{a}}) \cdot g \cdot h$, is the head correction, with ρ_{f} the density of the working fluid, ρ_{a} the air density, g the local acceleration due to gravity, and h the height difference between the reference levels of the two pressure balances (participant's standard and TS). h is positive if the level of the participant's standard is higher.

The effective area of TS (A'_{p}) at 20 °C can be calculated with the equation

$$A'_{\mathrm{p}} = \frac{\sum_i m'_i g\left(1 - \frac{\rho_{\mathrm{a}}}{\rho'_i}\right) + 2\sigma\sqrt{\pi A'_{0,\mathrm{nom}}}}{p'\left[1 + \left(\alpha'_{\mathrm{p}} + \alpha'_{\mathrm{c}}\right)\left(t' - t'_0\right)\right]} \,, \qquad (5.2)$$

where

m'_i are true masses of the piston, the mass loading bell and the mass pieces placed on the mass loading bell of TS;

ρ'_i are densities of the parts with masses m'_i;

ρ_{a} is air density;

g is local gravity acceleration;

σ is surface tension of the TS pressure transmitting medium (DOS);

$A'_{0,\mathrm{nom}}$ is nominal effective area of TS;

p' is pressure generated by the participant's standard at the TS reference level;

α'_{p} and α'_{c} are thermal expansion coefficients of the piston and cylinder materials, respectively;

t' is temperature of TS;

t'_0 is reference temperature, t'_0 = 20 °C.

The values of p', ρ_{a} and t' as well as the masses of the participant were calculated or measured by each participant. All other parameters were provided by the pilot institute.

The zero-pressure effective area of TS (A'_0) and its pressure distortion coefficient (λ') were also reported from the results of all 60 measurements, based on the equation below:

$$A'_p = A'_0(1+\lambda' p). \qquad (5.3)$$

The combined standard uncertainties of A'_0 and λ' as well as a description of calculation were included. Uncertainties were evaluated at a level of one standard uncertainty (coverage factor $k = 1$) based on the *Guide to the Expression of Uncertainty in Measurement* (GUM)[4].

The participants reported their results to the pilot institute, NMIJ/AIST, using the following sheets[7].

(i) Details of the participant's standard (Appendix A4)
(ii) Details of the measurement conditions (Appendix A5)
(iii) Results in individual cycles [1/3, 2/3, 3/3] (Appendix A6)
(iv) Summary of all cycles (Appendix A7)
(v) Calculated result of A'_0 and λ' (Appendix A8)
(vi) Uncertainty budget (using the participant's usual format).

5.4 Methods and parameters used by each participating institute

Details of the methods and parameters in each participant's measurement were reported and are listed in Table 5.1.

Table 5.1: Details of the parameters used by each participating institute. All the uncertainties are expressed as the standard ones.

i	Institute	Comparison method	Local gravity g_1			Height diff. H	
			Value [m/s^2]	Unc. [m/s^2]	Unc. [ppm]	Value [mm]	Unc. [mm]
1	NMIJ/AIST	Comparator method[14]	9.7994804	2.0E-06	0.20	< 12	0.5
2	NPLI	Fall-rate method	9.7912393	1.02E-05	1.04	0	0.5
3	NMC/A*STAR	Fall-rate method	9.7805553	1.8E-06	0.18	125.9	0.5
4	NIMT	Comparator method	9.7831243	5.65E-06	0.58	15.4	1.16
5	NMIA	Fall-rate method[15]	9.7994990	1.8E-06	0.18	1.3	0.4
6	NIM	Fall-rate method	9.801245	2E-06	0.20	0.05	1
7	CMS/ITRI	Fall-rate method	9.78913698	2.26E-06	0.23	0	1.0
8	KIM-LIPI	Fall-rate method	9.7813798	4.9E-06	0.50	0.19	0.06
9	KRISS	Fall-rate method	9.798310	2.5E-06	0.26	0.0	0.5

6. Results

6.1 Stability of transfer standard

The stability of the transfer standard, or the stability of the effective area of the piston-cylinder used, is evaluated from multiple calibration results conducted by the pilot institute. During the whole period, two calibrations are conducted for the piston-cylinder SN 1510, four calibrations for the piston-cylinder SN 1562, and four calibrations for the piston-cylinder SN 1648 by the pilot institute. Three cycles are repeated in each calibration. Figure 6.1 shows the relative deviation of each calibration results from the average for respective piston-cylinders. Although the range of deviation differs depending on each piston-cylinder, all the piston-cylinders do not show monotonous shift with time, showing that the transfer standard does not show long-term shift during the comparison period. Then, the scattering of the results seems to originate from the combined effect of short-term random errors and instability of the transfer standard. Also, the range of deviation does not depend on the pressure. Thus, the scattering of the results is treated as a rectangular distribution, and then, the uncertainty due to the instability of the transfer standard is estimated from the maximum value among the deviations divided by $2\sqrt{3}$. The maximum values of the deviation and the estimated uncertainties for respective piston-cylinders are listed in Table 6.1. These uncertainties are incorporated into the combined uncertainty for each participant, which will be explained in section 6.3.

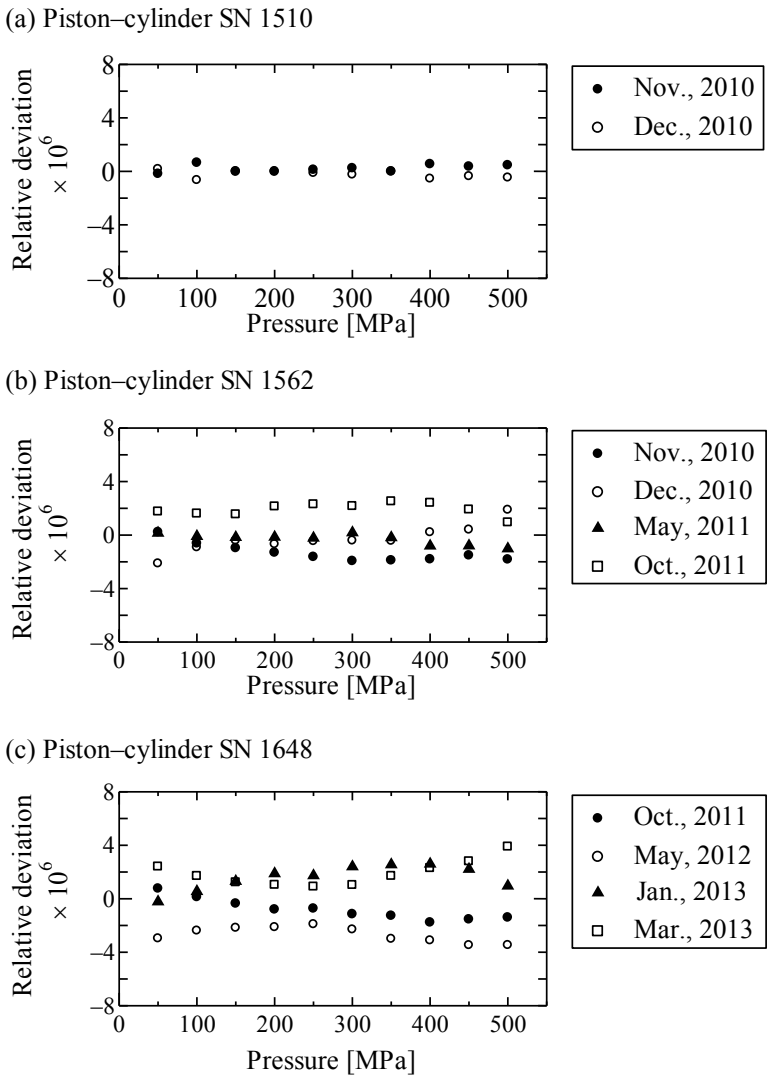

Figure 6.1: Stability of transfer standards. For each piston-cylinder, the relative deviations of each calibration results from the average are plotted against the measurement pressure.

Table 6.1 Maximum relative deviation and uncertainty due to the instability of the transfer standard for respective piston-cylinders.

	SN 1510 (j = 1)	SN 1562 (j = 2)	SN 1648 (j = 3)
Maximum relative deviation [10^{-6}]	1.3	4.4	7.4
Relative standard uncertainty [10^{-6}]	0.4	1.3	2.1
Standard uncertainty [mm^2]	7.8E-07	2.6E-06	4.1E-06

6.2 Results of participating institutes

Since all the piston-cylinders do not show monotonous or unidirectional shift with time, the results of the participants are directly compared in terms of the effective area at each calibration pressure without a drift correction. The results reported from participants are listed for respective piston-cylinders used, in sections 6.2.1 to 6.2.3. To compare the results all together, the relative deviations from the pilot institute's result are calculated in section 6.2.4.

6.2.1 Piston-cylinder SN 1510 (Petal 1)

Two participants, NMIJ/AIST and NPLI, measured the piston-cylinder SN 1510 in Petal 1. The result of the pilot institute is the average between the two calibration results performed on November and December in 2010, just before sending the transfer standard to NPLI. The reported results are listed in Table 6.2.

Table 6.2 Effective areas of piston-cylinder SN 1510.

i	1	2
j	1	1
Nom. Pres. [MPa]	NMIJ/AIST [mm^2]	NPLI [mm^2]
50	1.960913	1.960896
100	1.961000	1.960990
150	1.961081	1.961073
200	1.961162	1.961158
250	1.961245	1.961242
300	1.961328	1.961335
350	1.961413	1.961419
400	1.961498	1.961499
450	1.961587	1.961596
500	1.961675	1.961676
A'_0 [mm^2]	1.960828	1.960813
λ' [MPa^{-1}]	8.58E-07	8.82E-07

6.2.2 Piston-cylinder SN 1562 (Petal 2, 3)

Six participants in Petal 2 and Petal 3 measured the piston-cylinder SN 1562. The result of the pilot institute is the average between the two calibration results performed on May 2011, just before Petal 2, and October 2011, between Petal 2 and Petal 3. The reported results are listed in Table 6.3.

Table 6.3 Effective areas of piston-cylinder SN 1562.

i	1	3	4	5	6	7
j	2	2	2	2	2	2
Nom. Pres. [MPa]	NMIJ/AIST [mm^2]	NMC/A*STAR [mm^2]	NIMT [mm^2]	NMIA [mm^2]	NIM [mm^2]	CMS/ITRI [mm^2]
50	1.962187	1.9622151	1.962145	1.962200	1.962198	1.962209
100	1.962259	1.9622692	1.962220	1.962267	1.962260	1.962268
150	1.962330	1.9623267	1.962304	1.962342	1.962337	1.962338
200	1.962403	1.9623843	1.962380	1.962420	1.962411	1.962410
250	1.962475	1.9624455	1.962458	1.962498	1.962492	1.962476
300	1.962550	1.9625006	1.962535	1.962576	1.962573	
350	1.962623	1.9625712	1.962612	1.96266	1.962654	
400	1.962697	1.9626414	1.962687	1.96274	1.962737	
450	1.962774		1.962762	1.96281	1.962822	
500	1.962851		1.962834	1.96290	1.962905	
A'_0 [mm^2]	1.962110		1.962071	1.962114	1.962102	1.962136
λ' [MPa^{-1}]	7.50E-07		7.84E-07	7.90E-07	8.10E-07	6.9E-07

6.2.3 Piston-cylinder SN 1648 (Petal 4)

Four participants in Petal 4 measured the piston-cylinder SN 1648. The result of the pilot institute is the average between the two calibration results performed on May 2012 and January 2013. The reported results are listed in Table 6.4.

Table 6.4 Effective areas of piston-cylinder SN 1648.

i	1	8	9
j	3	3	3
Nom. Pres. [MPa]	NMIJ/AIST [mm^2]	KIM-LIPI [mm^2]	KRISS [mm^2]
50	1.960640	1.9606161	1.960657
100	1.960721	1.9606961	1.960731
150	1.960801	1.9607773	1.960800
200	1.960880	1.9608298	1.960867
250	1.960961	1.9608992	1.960936
300	1.961043	1.9609694	1.961009
350	1.961124	1.9610433	1.961084
400	1.961210	1.9611292	1.961162
450	1.961296	1.9612151	1.961242
500	1.961384	1.9613086	1.961324
A'_0 [mm^2]	1.960560	1.960537	1.960577
λ' [MPa^{-1}]	8.17E-07	7.62E-07	7.50E-07

6.2.4 Deviations of participants' results from the pilot institute's results

To simply compare the results among all the participants in this comparison, the relative deviations of the participants' results from the pilot institute's results were calculated as $(A_{p,i,j} - A_{p,i=1,j})/A_{p,i=1,j}$. The results thus obtained are listed in Table 6.5, and their graphical representations is shown in Fig. 6.2 in two vertical scales.

Table 6.5 Relative deviations of the participants' results from the pilot institute's results.

i	1	2	3	4	5	6	7	8	9
Nom. Pres. [MPa]	NMIJ/AIST [10^{-6}]	NPLI [10^{-6}]	NMC/ A*STAR [10^{-6}]	NIMT [10^{-6}]	NMIA [10^{-6}]	NIM [10^{-6}]	CMS/ITRI [10^{-6}]	KIM-LIPI [10^{-6}]	KRISS [10^{-6}]
50	0.0	-8.8	14.1	-21.6	6.4	5.4	11.0	-12.1	8.7
100	0.0	-5.5	5.0	-20.1	3.8	0.3	4.4	-12.8	5.0
150	0.0	-4.2	-1.6	-13.2	6.2	3.6	4.0	-11.9	-0.4
200	0.0	-2.3	-9.3	-11.5	8.9	4.3	3.7	-25.6	-6.7
250	0.0	-1.5	-15.2	-8.8	11.6	8.5	0.5	-31.4	-12.7
300	0.0	3.7	-24.9	-7.4	13.5	12.0		-37.4	-17.2
350	0.0	3.1	-26.5	-5.7	18.8	15.7		-41.3	-20.6
400	0.0	0.4	-28.3	-5.1	21.9	20.4		-41.0	-24.3
450	0.0	4.7		-6.0	18.5	24.6		-41.1	-27.4
500	0.0	0.5		-8.7	24.9	27.4		-38.5	-30.6

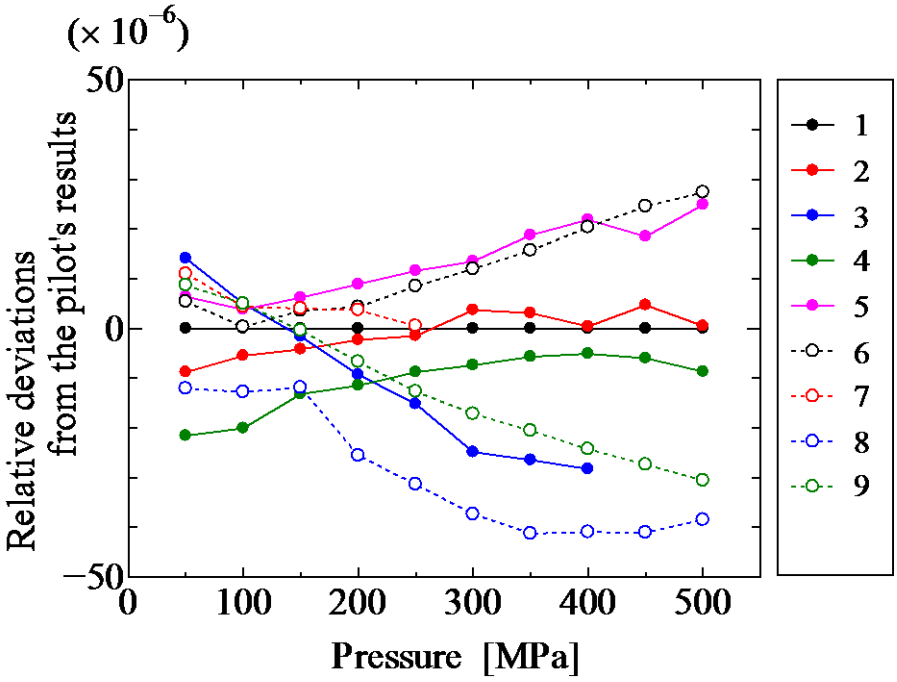

Figure 6.2: Relative deviations of the participants' results from the pilot institute's results.

6.3 Uncertainty

6.3.1 Uncertainty of the effective area of the transfer standard

In this section, all the uncertainties are expressed as the standard ones. The combined standard uncertainty of the effective area of the *j*-th piston-cylinder measured by the *i*-th participant, $u(A_{p,i,j})$, is estimated from the root-sum-square of two uncertainty factors, the uncertainty of the effective area of the transfer standard reported by each participant, $u\langle A'_{p,i,j}\rangle$, and the uncertainty due to the instability of the transfer standard, $u_{TS,i,j}$, as the following equation:

$$u\left(A_{p,i,j}\right)=\sqrt{u^2\left\langle A'_{p,i,j}\right\rangle+u^2_{TS,i,j}}\ . \qquad (6.1)$$

$u\langle A'_{p,i,j}\rangle$ reported by each participant includes all of the necessary uncertainty components based on equations (5.1) and (5.2). However, in the calculation of type A uncertainty, or the standard deviation of the six measurement results, some participants calculated a standard deviation of the average value, while others calculated a standard deviation of the distribution. To estimate and compare the participants' uncertainties consistently, the standard deviation of the distribution was recalculated by the pilot institute using the reported six measurement results at each measurement pressure. Table 6.6 lists the relative standard deviations for the three piston-cylinders measured at the pilot institute. Table 6.7 lists the standard deviations at the other participants. When the reported values by the participant differs from the recalculated ones, the reported values are also presented in parentheses. Then, the relative value of $u\langle A'_{p,i,j}\rangle$ is recalculated using the values in the table.

Table 6.6 Relative standard deviations for three piston-cylinders measured at the pilot institute

i	1	1	1
j	1	2	3
Nom. Pres. [MPa]	SN 1510 [10^{-6}]	SN 1562 [10^{-6}]	SN 1648 [10^{-6}]
50	2.2	2.9	2.8
100	1.2	4.1	3.2
150	0.7	4.1	2.9
200	0.8	3.9	2.7
250	0.7	3.2	2.3
300	0.9	2.4	2.2
350	0.8	2.0	2.8
400	1.2	1.8	3.2
450	1.0	1.7	3.7
500	1.0	1.4	3.8

Table 6.7 Relative standard deviations at the participants.

i	1	2	3	4	5	6	7	8	9
j	1	1	2	2	2	2	2	3	3
Nom. Pres. [MPa]	NMIJ/AIST [10^{-6}]	NPLI [10^{-6}]	NMC/ A*STAR [10^{-6}]	NIMT [10^{-6}]	NMIA [10^{-6}]	NIM [10^{-6}]	CMS/ITRI [10^{-6}]	KIM-LIPI [10^{-6}]	KRISS [10^{-6}]
50	2.2	3.3	2.8	5.0	2.0	1.8 (0.72)	3.2	5.1	3.7
100	1.2	4.0	4.3	3.3	3.2	0.8 (0.30)	4.9	5.3	2.9
150	0.7	4.8	4.8	1.3	4.5	2.0 (0.79)	4.2	3.6	2.4
200	0.8	3.0	8.9	1.2	4.4	1.6 (0.69)	2.7	5.0	3.2
250	0.7	1.8	7.8	0.9	5.2	1.3 (0.56)	0.2	3.4	3.2
300	0.9	2.2	3.5	0.7	3.1	0.8 (0.34)		4.4	2.4 (2.9)
350	0.8	1.2	3.9	0.6	2.8	0.4 (0.15)		2.6	2.2
400	1.2	1.2	3.4	1.2	2.8	0.6 (0.24)		2.2	1.6 (2.1)
450	1.0	2.4		1.0	2.6	0.5 (0.19)		1.8	1.8
500	1.0	1.3		3.4	0.0	1.0 (0.40)		1.5	1.5

The uncertainty due to the instability of the transfer standard $u_{\mathrm{TS},i,j}$ depends only on the piston-cylinder used. The values of $u_{\mathrm{TS},i,j}$ for respective piston-cylinders were listed in Table 6.1 in section 6.1.

The combined standard uncertainties are calculated from equation (6.1). The relative values against the pilot institute's results of respective piston-cylinders, $u(A_{\mathrm{p},i,j})$ / $A_{\mathrm{p},i=1,j}$, are listed in Table 6.8 and graphically shown in Fig.6.3 with two vertical scales.

Table 6.8 Relative standard uncertainty of the effective area $u(A_{\mathrm{p},i,j})$ / $A_{\mathrm{p},i=1,j}$.

i	1	2	3	4	5	6	7	8	9
j	1	1	2	2	2	2	2	3	3
Nom. Pres. [MPa]	NMIJ/AIST [10^{-6}]	NPLI [10^{-6}]	NMC/ A*STAR [10^{-6}]	NIMT [10^{-6}]	NMIA [10^{-6}]	NIM [10^{-6}]	CMS/ITRI [10^{-6}]	KIM-LIPI [10^{-6}]	KRISS [10^{-6}]
50	17	41	25	21	12	20	38	23	20
100	17	41	28	23	13	20	38	24	21
150	19	41	32	27	16	22	38	28	22
200	20	41	39	31	19	24	38	32	24
250	22	41	43	36	22	27	38	37	26
300	25	41	48	42	25	30		42	29
350	27	41	54	46	29	33		47	31
400	30	41	61	52	32	36		52	34
450	33	41		56	36	40		57	37
500	37	41		62	39	44		62	40

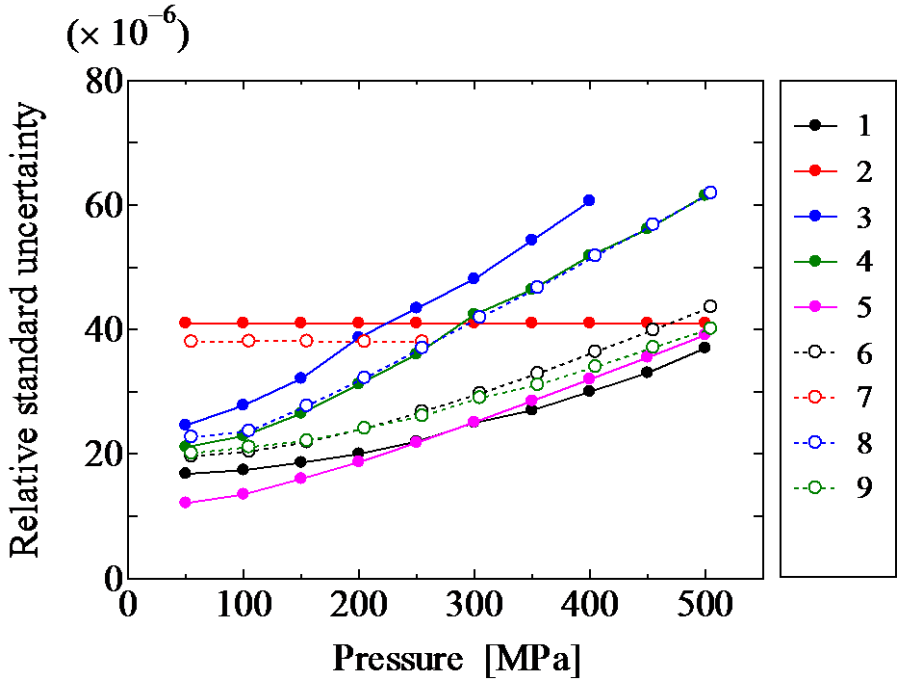

Figure 6.3 Relative standard uncertainty of the effective area of the transfer standard

6.3.2 Reported uncertainty components (Informative)

Principal uncertainty components were also separately reported in the form of Appendix A7 in the protocol. Table 6.9 presents the relative standard uncertainty of p', which includes uncertainty of pressure generated by the participant's standard, the uncertainty of the height difference, the density of the pressure transmitting medium, and so forth.

Table 6.9 Relative standard uncertainty of p' in 10^{-6}.

i	1	2	3	4	5	6	7	8	9
j	1	1	2	2	2	2	2	3	3
Nom. Pres. [MPa]	NMIJ/AIST [10^{-6}]	NPLI [10^{-6}]	NMC/ A*STAR [10^{-6}]	NIMT [10^{-6}]	NMIA [10^{-6}]	NIM [10^{-6}]	CMS/ITRI [10^{-6}]	KIM-LIPI [10^{-6}]	KRISS [10^{-6}]
50	16.1	40	2.3	20.2	11.9	19.2	37	18.9	18
100	16.8	40	4.5	22.2	13.3	20.0	37	21.4	19
150	18.0	40	5.5	25.9	15.7	21.6	37	25.7	20
200	19.6	40	10.0	30.7	18.5	23.8	37	30.4	22
250	21.5	40	8.3	35.6	21.7	26.5	37	35.3	25
300	23.8	40	2.5	42.0	25.0	29.5		40.3	27
350	26.4	40	2.8	46.0	28.4	32.8		45.3	30
400	29.3	40	2.1	51.5	31.9	36.2		50.4	33
450	32.5	40		55.8	35.5	39.8		55.5	36
500	36.0	40		61.2	39.0	43.5		60.6	39

Table 6.10 presents the standard uncertainty of the temperature of the transfer standard, which were treated as the type B uncertainty of the temperature measurement on the transfer standard.

Table 6.10 Standard uncertainty of t' in temperature (K).

i	1	2	3	4	5	6	7	8	9
j	1	1	2	2	2	2	2	3	3
Nom. Pres. [MPa]	NMIJ/AIST [10^{-6}]	NPLI [10^{-6}]	NMC/ A*STAR [10^{-6}]	NIMT [10^{-6}]	NMIA [10^{-6}]	NIM [10^{-6}]	CMS/ITRI [10^{-6}]	KIM-LIPI [10^{-6}]	KRISS [10^{-6}]
50	0.2	0.12	0.03	0.15	0.16	0.2	0.02	0.01	0.2
100	0.2	0.12	0.03	0.15	0.16	0.2	0.02	0.01	0.2
150	0.2	0.12	0.03	0.15	0.16	0.2	0.02	0.01	0.2
200	0.2	0.12	0.03	0.15	0.16	0.2	0.02	0.01	0.2
250	0.2	0.12	0.03	0.15	0.16	0.2	0.02	0.01	0.2
300	0.2	0.12	0.03	0.15	0.16	0.2		0.01	0.2
350	0.2	0.12	0.03	0.15	0.16	0.2		0.01	0.2
400	0.2	0.12	0.03	0.15	0.16	0.2		0.01	0.2
450	0.2	0.12		0.15	0.16	0.2		0.01	0.2
500	0.2	0.12		0.15	0.16	0.2		0.01	0.2

7. Linking of the results to CCM.P-K13 reference values

The results of the participants in APMP.M.P-K13 are linked to those of CCM.P-K13 through the results of the two linking laboratories, NMIJ and NPLI. The deviations of the *i*-th participant's results from the CCM.P-K13 reference values, $\Delta A_{p,i,\mathrm{ref}}$, are calculated by the following equation[16, 17]:

$$\Delta A_{\mathrm{p},i,\mathrm{ref}} = A_{\mathrm{p},i,j} + \Delta A_{\mathrm{p,TS},j} + \Delta A_{\mathrm{p,Link}} - A_{\mathrm{p,ref}}\,, \qquad (7.1)$$

where $A_{\mathrm{p},i,j}$ is the effective area measured by each participant (reported in section 6.2), $\Delta A_{\mathrm{p,TS},j}$ is the correction for the difference in the effective areas between the piston-cylinders used in APMP.M.P-K13, $\Delta A_{\mathrm{p,Link}}$ is the correction for the linkage between APMP.M.P-K13 and CCM.P-K13 deduced from the results of the two linking laboratories, $A_{\mathrm{p,ref}}$ is the key comparison reference value of CCM.P-K13[4]. Accordingly, the combined standard uncertainty of $\Delta A_{\mathrm{p},i,\mathrm{ref}}$ is evaluated by the following equation[16, 17],

$$u_c\left(\Delta A_{\mathrm{p},i,\mathrm{ref}}\right) = \sqrt{u^2\left(A_{\mathrm{p},i,j}\right) + u^2\left(\Delta A_{\mathrm{p,TS},j}\right) + u^2\left(\Delta A_{\mathrm{p,Link}}\right) + u^2\left(A_{\mathrm{p,ref}}\right)}. \qquad (7.2)$$

The effective areas measured by each participant, $A_{\mathrm{p},i,j}$, the first term in the right-hand side of (7.1), were listed in Table 6.2, 6.3, and 6.4. The uncertainties $u(A_{\mathrm{p},i,j})$ were calculated as described in section 6.3.1, and the absolute values are listed in Table 7.1.

Table 7.1 Standard uncertainty of the effective area $u(A_{\mathrm{p},i,j})$

i	1	2	3	4	5	6	7	8	9
j	1	1	2	2	2	2	2	3	3
Nom. Pres. [MPa]	NMIJ/AIST [mm²]	NPLI [mm²]	NMC/ A*STAR [mm²]	NIMT [mm²]	NMIA [mm²]	NIM [mm²]	CMS/ITRI [mm²]	KIM-LIPI [mm²]	KRISS [mm²]
50	0.000033	0.000080	0.000048	0.000041	0.000024	0.000038	0.000075	0.000045	0.000039
100	0.000034	0.000080	0.000055	0.000045	0.000026	0.000040	0.000075	0.000046	0.000041
150	0.000036	0.000080	0.000063	0.000052	0.000031	0.000043	0.000075	0.000054	0.000043
200	0.000039	0.000080	0.000076	0.000061	0.000037	0.000047	0.000075	0.000063	0.000047
250	0.000043	0.000080	0.000085	0.000071	0.000043	0.000053	0.000075	0.000072	0.000051
300	0.000049	0.000080	0.000094	0.000083	0.000049	0.000058		0.000082	0.000057
350	0.000053	0.000080	0.000107	0.000091	0.000056	0.000065		0.000092	0.000061
400	0.000059	0.000080	0.000119	0.000102	0.000063	0.000071		0.000102	0.000067
450	0.000065	0.000080		0.000110	0.000070	0.000078		0.000111	0.000073
500	0.000073	0.000080		0.000121	0.000077	0.000086		0.000121	0.000079

The second term in the right-hand side of (7.1), $\Delta A_{\mathrm{p,TS},j}$, provides the correction for the difference in the effective areas of different transfer standards used in APMP.M.P-K13. Among three piston-cylinders used in APMP.M.P-K13, the results of the piston-cylinder SN 1510 (j = 1) is used for the linkage to CCM.P-K13, because SN 1510 is the

only piston-cylinder whose effective area was measured by both the linking laboratories. For the other piston-cylinders, SN 1562 (j = 2) and SN 1648 (j = 3), the deviation of the effective area from SN 1510 is corrected by this term. Specifically, the value of $\Delta A_{\mathrm{p,TS},j}$, and its uncertainty $u(\Delta A_{\mathrm{p,TS},j})$, are calculated from the pilot institute's results, as the following.

In the case of j = 1, $\Delta A_{\mathrm{p,TS},j} = 0$, (7.3)

$u(\Delta A_{\mathrm{p,TS},j}) = 0$, (7.4)

In the case of j = 2 or 3, $\Delta A_{\mathrm{p,TS},j} = A_{\mathrm{p},i=1,j=1} - A_{\mathrm{p},i=1,j}$, (7.5)

$$u\left(\Delta A_{\mathrm{p,TS},j}\right) = \sqrt{u_A^2\left(A_{\mathrm{p},i=1,j=1}\right) + u_A^2\left(A_{\mathrm{p},i=1,j}\right)}. \quad (7.6)$$

In the second case (j = 2 or 3), the uncertainty of this correction is calculated from the type A uncertainties in the measurements of respective piston-cylinders at the pilot institute. It is due to the fact that the uncertainty components related to the pilot institute's standard and the measurement conditions are considered to be fully correlated between the three effective areas $A_{\mathrm{p},i=1,j}$. The type A uncertainties for the three piston-cylinders were evaluated in section 6.3 and listed in Table 6.6. Then, the calculated values of $\Delta A_{\mathrm{p,TS},j}$ and their uncertainties are listed in Table 7.2.

Table 7.2 Values of $\Delta A_{\mathrm{p,TS},j}$ and their uncertainties for respective piston-cylinders

j	1		2		3	
Nom. Pres. [MPa]	$\Delta A_{\mathrm{p,TS},j=1}$ [mm^2]	$u(\Delta A_{\mathrm{p,TS},j=1})$ [mm^2]	$\Delta A_{\mathrm{p,TS},j=2}$ [mm^2]	$u(\Delta A_{\mathrm{p,TS},j=2})$ [mm^2]	$\Delta A_{\mathrm{p,TS},j=3}$ [mm^2]	$u(\Delta A_{\mathrm{p,TS},j=3})$ [mm^2]
50	0	0	-0.001274	0.000007	0.000273	0.000007
100	0	0	-0.001259	0.000008	0.000279	0.000007
150	0	0	-0.001249	0.000008	0.000281	0.000006
200	0	0	-0.001240	0.000008	0.000282	0.000005
250	0	0	-0.001231	0.000006	0.000284	0.000005
300	0	0	-0.001221	0.000005	0.000285	0.000005
350	0	0	-0.001210	0.000004	0.000289	0.000006
400	0	0	-0.001199	0.000004	0.000289	0.000007
450	0	0	-0.001187	0.000004	0.000291	0.000007
500	0	0	-0.001177	0.000003	0.000291	0.000008

The third term in the right-hand side of (7.1), $\Delta A_{\mathrm{p,Link}}$, represents the difference between the effective areas of the transfer standard SN 1510 used in APMP.M.P-K13 and of the transfer standard (DH-Budenberg, 4603) used in CCM.P-K13. The difference is deduced by the linking laboratories' results in the both comparisons. Concrete calculations for $\Delta A_{\mathrm{p,Link}}$ are as the following:

$$\Delta A_{\mathrm{p,Link}} = \sum_{i=1}^{2} \frac{\Delta A_{\mathrm{p,Link}\,i}}{u^2(\Delta A_{\mathrm{p,Link}\,i})} \Bigg/ \sum_{i=1}^{2} \frac{1}{u^2(\Delta A_{\mathrm{p,Link}\,i})} \tag{7.7}$$

$$u^2(\Delta A_{\mathrm{p,Link,}}) = 1 \Bigg/ \sum_{i=1}^{2} \frac{1}{u^2(\Delta A_{\mathrm{p,Link}\,i})} \quad , \tag{7.8}$$

where $\Delta A_{\mathrm{p,Link},1} = A_{\mathrm{p},i=1,\mathrm{CCM}} - A_{\mathrm{p},i=1,j=1}$, (7.9)

$$\Delta A_{\mathrm{p,Link},2} = A_{\mathrm{p},i=2,\mathrm{CCM}} - A_{\mathrm{p},i=2,j=1}\,, \tag{7.10}$$

$$u^2(\Delta A_{\mathrm{p,Link},1}) = u_A^2(A_{\mathrm{p},i=1,\mathrm{CCM}}) + u_A^2(A_{\mathrm{p},i=1,\,j=1})\,, \tag{7.11}$$

$$u^2(\Delta A_{\mathrm{p,Link},2}) = u_A^2(A_{\mathrm{p},i=2,\mathrm{CCM}}) + u_A^2(A_{\mathrm{p},i=2,\,j=1})\,. \tag{7.12}$$

In equations (7.9) and (7.10), $\Delta A_{\mathrm{p,Link},i,}$ represents a linking invariant for each linking laboratory, i =1 for NMIJ/AIST, and i = 2 for NPLI. The value of $\Delta A_{\mathrm{p,Link},i}$ is calculated as the difference of the effective area between SN 1510 and CCM.P-K13 transfer standard. NMIJ/AIST and NPLI used the same standard devices with the same uncertainty for the two comparisons. The measurement methods and the basic properties of piston-cylinders used as the transfer standard are also identical. Thus, considering the correlation between the two comparisons, the uncertainty of the difference $\Delta A_{\mathrm{p,Link},i}$, in (7.11) and (7.12) is estimated from the combination of the type A uncertainties at respective measurements for CCM.P-K13 and APMP.M.P-K13 comparisons. Then, the linking invariant, $\Delta A_{\mathrm{p,Link}}$ in (7.7), is calculated by the inverse-variance weighted mean of the invariants for the respective linking laboratories. The associated standard uncertainty of the inverse-variance weighted mean of the linking invariant is calculated by (7.8). The values of the invariants, $\Delta A_{\mathrm{p,Link},i}$ and $\Delta A_{\mathrm{p,Link}}$, are listed in Table 7.3 with their uncertainties.

Table 7.3 Values of the linking invariants $\Delta A_{\mathrm{p,Link},i}$ and $\Delta A_{\mathrm{p,Link}}$ with their uncertainties

	i = 1 (NMIJ/AIST)		i = 2 (NPLI)		Linking invariant	
Nom. Pres.	$\Delta A_{\mathrm{p,Link},i=1}$	$u(\Delta A_{\mathrm{p,Link},i=1})$	$\Delta A_{\mathrm{p,Link},i=2}$	$u(\Delta A_{\mathrm{p,Link},i=2})$	$\Delta A_{\mathrm{p,Link}}$	$u(\Delta A_{\mathrm{p,Link}})$
[MPa]	[mm^2]	[mm^2]	[mm^2]	[mm^2]	[mm^2]	[mm^2]
50	0.000239	0.000007	0.000208	0.000024	0.000237	0.000007
100	0.000269	0.000005	0.000254	0.000013	0.000267	0.000005
150	0.000305	0.000003	0.000303	0.000017	0.000305	0.000003
200	0.000333	0.000003	0.000335	0.000017	0.000333	0.000003
250	0.000352	0.000002	0.000361	0.000013	0.000353	0.000002
300	0.000364	0.000003	0.000370	0.000017	0.000364	0.000003
350	0.000369	0.000002	0.000383	0.000015	0.000369	0.000002
400	0.000373	0.000003	0.000388	0.000012	0.000374	0.000003
450	0.000369	0.000004	0.000391	0.000017	0.000370	0.000004
500	0.000366	0.000002	0.000417	0.000017	0.000367	0.000002

The fourth term in the right-hand side of (7.1), $A_{\mathrm{p,ref}}$, represents the key comparison reference value of CCM.P-K13. The values of $A_{\mathrm{p,ref}}$ and their uncertainties, obtained from the final report of CCM.P-K13[4], are listed in Table 7.4.

Table 7.4 Key comparison reference values of CCM.P-K13 with their uncertainties.

Nom. Pres.	$A_{\mathrm{p,ref}}$	$u(A_{\mathrm{p,ref}}) / A_{\mathrm{p,ref}}$	$u(A_{\mathrm{p,ref}})$
[MPa]	[mm^2]	[10^{-6}]	[mm^2]
50	1.961152	13.5	0.000026
100	1.961269	4.6	0.000009
150	1.961386	3.4	0.000007
200	1.961495	3.4	0.000007
250	1.961597	5.4	0.000011
300	1.961692	5.9	0.000012
350	1.961782	7.7	0.000015
400	1.961871	6.7	0.000013
450	1.961956	8.8	0.000017
500	1.962041	11.1	0.000022

The deviations of the participants' results from the CCM.P-K13 reference values, $\Delta A_{p,i,\mathrm{ref}}$, calculated by (7.1) using the components described above, are listed in Table 7.5. Also, the combined standard uncertainty calculated by (7.2) is listed in Table 7.6.

Table 7.5 Deviations of the participants' results from the CCM.P-K13 reference values, $\Delta A_{p,i,\mathrm{ref}}$, calculated by (7.1).

i	1	2	3	4	5	6	7	8	9
j	1	1	2	2	2	2	2	3	3
Nom. Pres. [MPa]	NMIJ/AIST [mm^2]	NPLI [mm^2]	NMC/ A*STAR [mm^2]	NIMT [mm^2]	NMIA [mm^2]	NIM [mm^2]	CMS/ITRI [mm^2]	KIM-LIPI [mm^2]	KRISS [mm^2]
50	-0.000002	-0.000020	0.000025	-0.000045	0.000010	0.000008	0.000019	-0.000026	0.000015
100	-0.000002	-0.000013	0.000008	-0.000041	0.000006	-0.000001	0.000007	-0.000027	0.000008
150	0.000000	-0.000008	-0.000003	-0.000026	0.000012	0.000007	0.000008	-0.000023	-0.000001
200	0.000000	-0.000004	-0.000018	-0.000022	0.000018	0.000009	0.000007	-0.000050	-0.000013
250	0.000000	-0.000003	-0.000029	-0.000017	0.000023	0.000017	0.000001	-0.000061	-0.000025
300	0.000000	0.000007	-0.000049	-0.000014	0.000027	0.000024		-0.000073	-0.000034
350	0.000000	0.000006	-0.000052	-0.000011	0.000037	0.000031		-0.000081	-0.000040
400	0.000001	0.000002	-0.000055	-0.000009	0.000044	0.000041		-0.000079	-0.000047
450	0.000001	0.000010		-0.000011	0.000037	0.000049		-0.000080	-0.000053
500	0.000001	0.000002		-0.000016	0.000050	0.000055		-0.000075	-0.000059

Table 7.6 Combined standard uncertainty of $\Delta A_{\mathrm{p},i,\mathrm{ref}}$ calculated by (7.2).

i	1	2	3	4	5	6	7	8	9
j	1	1	2	2	2	2	2	3	3
Nom. Pres. [MPa]	NMIJ/AIST [mm^2]	NPLI [mm^2]	NMC/ A*STAR [mm^2]	NIMT [mm^2]	NMIA [mm^2]	NIM [mm^2]	CMS/ITRI [mm^2]	KIM-LIPI [mm^2]	KRISS [mm^2]
50	0.000043	0.000085	0.000056	0.000050	0.000036	0.000047	0.000080	0.000052	0.000048
100	0.000036	0.000081	0.000056	0.000047	0.000029	0.000042	0.000076	0.000048	0.000043
150	0.000037	0.000081	0.000064	0.000053	0.000033	0.000044	0.000075	0.000055	0.000044
200	0.000040	0.000081	0.000077	0.000062	0.000038	0.000048	0.000075	0.000064	0.000048
250	0.000044	0.000081	0.000086	0.000072	0.000045	0.000054	0.000076	0.000073	0.000052
300	0.000050	0.000081	0.000095	0.000084	0.000051	0.000060		0.000083	0.000058
350	0.000055	0.000082	0.000108	0.000092	0.000058	0.000067		0.000093	0.000063
400	0.000060	0.000082	0.000120	0.000103	0.000064	0.000073		0.000103	0.000068
450	0.000067	0.000082		0.000112	0.000072	0.000080		0.000113	0.000075
500	0.000076	0.000083		0.000123	0.000080	0.000088		0.000124	0.000082

Finally, the degree of equivalence of the participants are expressed by the relative deviations of the participants' results from CCM.P-K13 reference values and the expanded ($k = 2$) relative uncertainties of these deviations. The results calculated by the following equations are shown in Table 7.6 and Table 7.7, and are also graphically shown in Fig. 7.1.

$$\Delta A_{\mathrm{p},i,\mathrm{ref}} / A_{\mathrm{p,ref}} = \left(A_{\mathrm{p},i,j} + \Delta A_{\mathrm{p,TS},j} + \Delta A_{\mathrm{p,Link}} - A_{\mathrm{p,ref}}\right) / A_{\mathrm{p,ref}} , \qquad (7.13)$$

$$U_c\left(\Delta A_{\mathrm{p},i,\mathrm{ref}} / A_{\mathrm{p,ref}}\right) = 2 \cdot u_c\left(\Delta A_{\mathrm{p},i,\mathrm{ref}}\right) / A_{\mathrm{p,ref}} . \qquad (7.14)$$

Table 7.7 Relative deviations of the participants' results from the CCM.P-K13 reference values, $\Delta A_{p,i,\mathrm{ref}}/A_{p,\mathrm{ref}}$, calculated by (7.13).

i	1	2	3	4	5	6	7	8	9
j	1	1	2	2	2	2	2	3	3
Nom. Pres. [MPa]	NMIJ/AIST [10^{-6}]	NPLI [10^{-6}]	NMC/ A*STAR [10^{-6}]	NIMT [10^{-6}]	NMIA [10^{-6}]	NIM [10^{-6}]	CMS/ITRI [10^{-6}]	KIM-LIPI [10^{-6}]	KRISS [10^{-6}]
50	-1.2	-10.0	12.9	-22.8	5.2	4.2	9.8	-13.3	7.5
100	-1.0	-6.5	4.0	-21.1	2.8	-0.7	3.3	-13.8	4.0
150	0.0	-4.2	-1.7	-13.2	6.1	3.6	3.9	-12.0	-0.4
200	0.0	-2.3	-9.3	-11.4	9.0	4.4	3.7	-25.6	-6.6
250	0.1	-1.3	-15.0	-8.7	11.7	8.7	0.6	-31.3	-12.5
300	0.1	3.7	-24.9	-7.3	13.6	12.1		-37.3	-17.2
350	0.2	3.3	-26.3	-5.5	19.0	15.9		-41.1	-20.4
400	0.5	0.9	-27.8	-4.6	22.4	20.9		-40.4	-23.7
450	0.5	5.3		-5.5	19.0	25.1		-40.6	-26.9
500	0.4	1.0		-8.3	25.3	27.9		-38.0	-30.2

Table 7.8 Expanded (k = 2) relative uncertainty of the relative deviations of the participants' results from the CCM.P-K13 reference values, calculated by (7.14).

i	1	2	3	4	5	6	7	8	9
j	1	1	2	2	2	2	2	3	3
Nom. Pres. [MPa]	NMIJ/AIST [10^{-6}]	NPLI [10^{-6}]	NMC/ A*STAR [10^{-6}]	NIMT [10^{-6}]	NMIA [10^{-6}]	NIM [10^{-6}]	CMS/ITRI [10^{-6}]	KIM-LIPI [10^{-6}]	KRISS [10^{-6}]
50	44	87	57	51	37	48	81	53	49
100	36	83	57	48	30	43	77	49	44
150	38	82	65	54	34	45	77	56	45
200	41	82	78	63	39	49	77	65	49
250	45	83	88	73	45	55	77	75	53
300	51	83	97	86	52	61		85	59
350	56	83	110	94	59	68		95	64
400	62	83	122	105	66	74		105	70
450	68	84		114	73	82		115	77
500	77	85		125	81	90		126	83

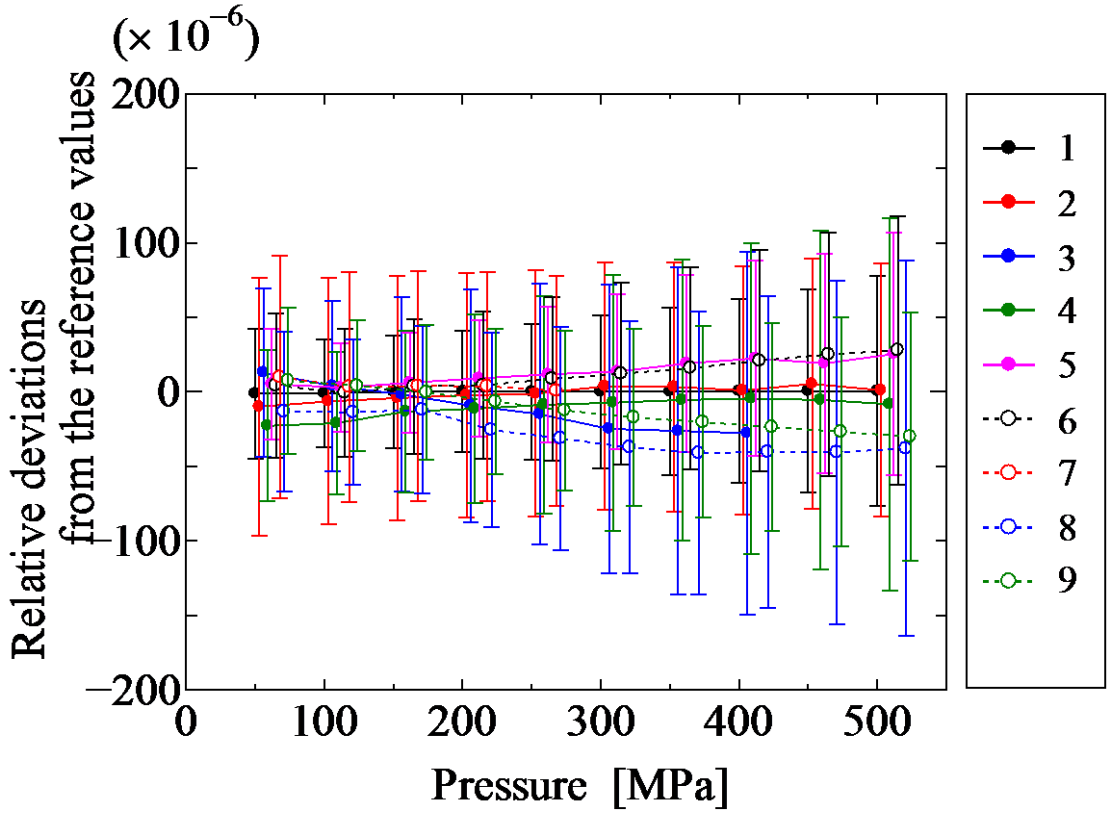

Figure 7.1: Relative deviations of the participants' results from the reference values of CCM.P-K13. Error bar represents expanded (k=2) uncertainty of the relative deviation.

8. Discussions

Monitoring data during TS transportations revealed that, in some places, temperature and humidity exceeds the expected permissible ranges, and relatively large impacts were applied mainly at airports. Fortunately, however, severe damages were not applied on the transfer standard, and changes in the characteristics of the piston-cylinder were not observed during the whole comparison. Then, these data are used just for checking the conditions during transportations. However, if the transfer standard did not work well, or characteristics of the transfer standard was changed during a comparison, such monitoring data would help to identify whether or when it is badly treated during transportation.

As explained in section 6.1, all the piston-cylinders used as the transfer standard did not show monotonous shift in their effective areas during the whole measurement period, showing a satisfactory long-term stability. This characteristic partly comes from the material for the piston-cylinder assembly; both the piston and cylinder were made from tungsten carbide. The uncertainty due to the instability intrinsic to each piston-cylinder, evaluated from multiple calibration results at the pilot institute, was relatively a few parts per million, and found to be uninfluential to the total uncertainty. Also, hysteresis of the TS piston-cylinder was not conspicuously observed in the pilot institute's results. Then, the measurement results in pressure increasing and decreasing processes were not distinguished with one another, then consequently, total six repeated data in three cycles were averaged to be the measurement result at each measurement pressure. The same analysis was applied to the participants whose maximum pressure was lower than 500 MPa.

To consistently evaluate the data scattering (type A uncertainty), the standard deviation (SD) of the distribution among the six results were recalculated by the pilot institute. The recalculated SDs for NIM and KRISS are only slightly different from those claimed by them, and then, the effect on the total uncertainty was negligible.

Linking to CCM.P-K13 was conducted through the difference in the effective areas between the piston-cylinder SN 1510 used in APMP.M.P-K13 and the piston-cylinder 4603 (DH-Budenberg) used in CCM.P-K13, because SN 1510 is the only piston-cylinder whose effective area is measured by both the linking laboratories. For the participants who measured other piston-cylinders (SN 1562 and SN 1648), additional uncertainty factor $u(\Delta A_{\mathrm{p,TS},j})$ was added, as shown in equation (7.2), but the value of $u(\Delta A_{\mathrm{p,TS},j})$ was relatively small, only a few parts per million, and almost negligible compared with the total uncertainty.

In the linking to CCM.P-K13, most of the uncertainty factors can be considered to be correlated between the measurements at the two comparisons CCM.P-K13 and APMP.M.P-K13 made by each linking laboratory. Then, only the type A uncertainties in CCM.P-K13 and APMP.M.P-K13 were used to evaluate the uncertainty of the linking invariant. In principle, the covariance between $\Delta A_{\mathrm{p,TS},j}$ and $\Delta A_{\mathrm{p,Link}}$ in equation (7.1) should be taken into consideration, because $\Delta A_{\mathrm{p},i=1,\ j=1}$ appears in the both terms. In practice, however, the calculated values of the covariance were negligibly small, and then explicit formulation was not described in the report.

Some participants claimed their uncertainty as a constant value, others claimed as an increasing functions of pressure. The relative combined (k=2) uncertainties of the deviation from the reference value ranges from 37 ppm to 87 ppm at 50 MPa, and from 77 ppm to 126 ppm at 500 MPa. These uncertainty values are comparable with those reported by the CCM.P-K13 participants.

9. Conclusions

The regional key comparison APMP.M.P-K13 was conducted to compare the performance of hydraulic pressure standards in the pressure range from 50 MPa to 500 MPa in a gauge mode. A set of pressure balance with a free-deformational piston-cylinder assembly was used as the transfer standard. Three piston-cylinder assemblies, only one at a time, were used to complete the measurements in the period from November 2010 to January 2013. The pressure-dependent effective areas of the transfer standard at specified pressures were reported by ten participants. Since one of the participants withdrew its results, the measurement results of the nine participants were finally compared. The measurement results were linked to the CCM.P-K13 reference values through the results of two linking laboratories, NMIJ/AIST and NPLI. Then, the deviations of the participants' results from the CCM.P-K13 reference values $\Delta A_{\mathrm{p},i,\mathrm{ref}}$ were calculated. The uncertainty of $\Delta A_{\mathrm{p},i,\mathrm{ref}}$ was evaluated by combining uncertainty of the effective area claimed by the participants, the uncertainty due to the instability of the transfer standard, uncertainty due to the linking to the reference value, and the uncertainty of the reference value. The results of all the nine participants agree with the CCM.P-K13 reference values within their expanded (k=2) uncertainties in the entire pressure range from 50 MPa to 500 MPa.

Acknowledgements

We would like to show our deep appreciation to Fluke Calibration for letting us use the set of pressure balance, including three piston-cylinders, throughout this comparison for more than two years. The invaluable advices and supports by Dr. A. K. Bandyopadhyay (NPLI), Dr. S. Y. Woo (KRISS), Dr. J. C. Torres-Guzman, the present Chairperson of the High Pressure Working Group (WGHP) of CCM, Dr. H. Tanaka, and Dr. K. Shirono, (Metrological Information Section, NMIJ) are gratefully acknowledged. Contributions by the staffs at the participating institutes are also appreciated.

References

1. Mutual recognition of national measurements standards and of calibration and measurement certificates issued by national metrology institutes (MRA), Technical Report, International Committee for Weights and Measures, 1999 (http://www.bipm.org/pdf/mra.pdf)
2. Guidelines for CIPM key comparisons, Appendix F to Mutual recognition of national measurements standards and of calibration and measurement certificates issued by national metrology institutes, Technical Report, International Committee for Weights and Measures, 1999 (http://www.bipm.org/pdf/guidelines.pdf)
3. Formalities required for the CCM key comparisons (2nd revised draft), 2001.
4. W. Sabuga, *et al*., Final report on key comparison CCM.P-K13 in the range 50 MPa to 500 MPa of hydraulic gauge pressure, *Metrologia* **49** 07006, 2012.
5. ISO/IEC 2008 Guide 98-3 Guide to the Expression of Uncertainty in Measurement (GUM: 1995), (Geneva, International Organization for Standardization), 2008.
6. Entering the details and results of RMO key and supplementary comparisons into the BIPM key comparison database, 2000.
7. T. Kobata and H. Kajikawa, Protocol of "Asia-Pacific Metrology Program 500 MPa Hydraulic Pressure Interlaboratory Comparison, APMP.M.P-K13, Edition 1.0 on November 2010 to Edition 1.5 on June 2012
8. H. Kajikawa, T. Kobata and A. Ooiwa, Features of a New Controlled-clearance Pressure Balance and *In Situ* Mass Calibration of Its Weights, *Trans. Soc. Instrum. Control Eng.* **44** (2008) 219-226
9. P. L. M. Heydemann and B. E. Welch, Experimental Thermodynamics, Vol. II, Chapter 4, Part 3, 147-202, International Union of Pure and Applied Chemistry, London, 1975.

10. H. Kajikawa, K. Ide and T. Kobata, Precise determination of the pressure distortion coefficient of new controlled-clearance piston-cylinders based on the Heydemann-Welch model, *Rev. Sci. Instrum.* **80** (2009) 095101
11. Y. Yang, J.Yue, Calculation of effective area for the NIM primary pressure standards, *PTB-Mitteilungen*, **121** (3) (2011) 266-269
12. Fluke Corporation, DH Instruments Division, PG7000™ PISTON GAUGES PG7102™, PG7202™, PG7302™, PG7601™ (Ver. 3.0 and Higher) Operation and Maintenance Manual.
(http://www.dhinstruments.com/supp1/manuals/pg7000/3152117_550099q.pdf)
13. Michael Bair and Pierre Delajoud, UNCERTAINTY ANALYSIS FOR PRESSURE DEFINED BY A PG7601, PG7102, PG7202 OR PG7302 PISTON GAUGE, 05 JUN 29.
14. T. Kobata and D. A. Olson, Accurate determination of equilibrium state between two pressure balances using a pressure transducer, *Metrologia* **42** (2005) S231-S234
15. C. M. Sutton, M. P. Fitzgerald, and W. Giardini, A method of analysis for cross-floats between pressure balances, *Metrologia* **42** (2005) S212-S215
16. J. E. Decker, A. G. Steele, and R. J. Douglas, Measurement science and the linking of CIPM and regional key comparisons, *Metrologia* **45** (2008) 223-232
17. Private communication with Dr. H. Tanaka, and Dr. K. Shirono, experts in statistics and uncertainty evaluation, in the Metrological Information Section in NMIJ/AIST.

Appendix: Relative deviations of the participants' results from the CCM.P-K13 reference values, and the expanded (k=2) uncertainties

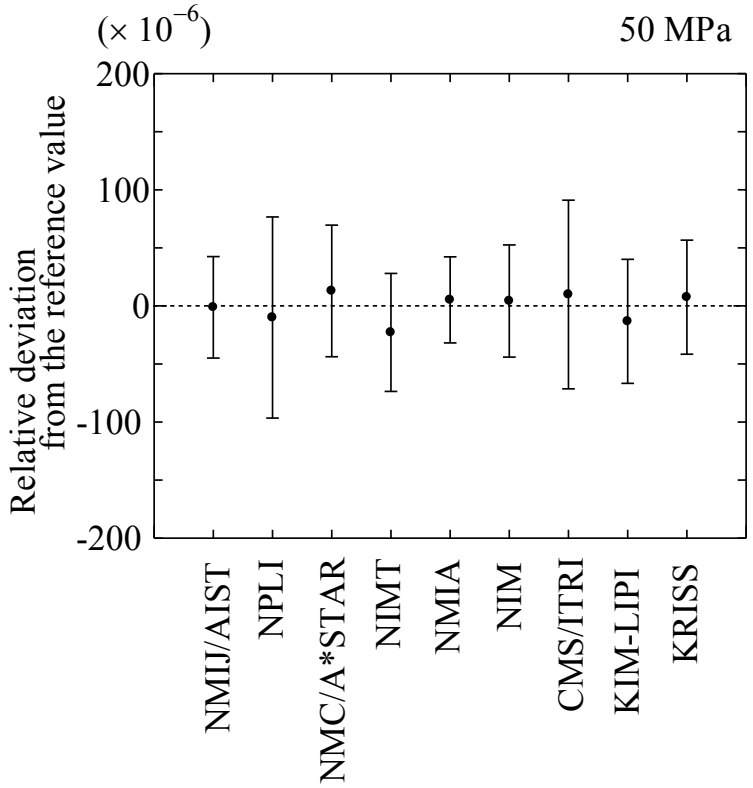

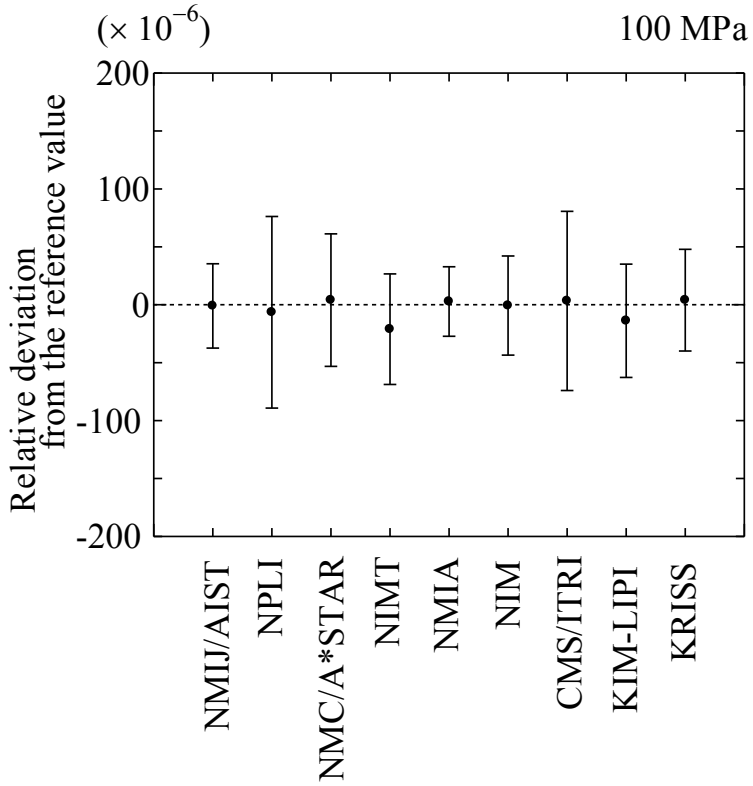

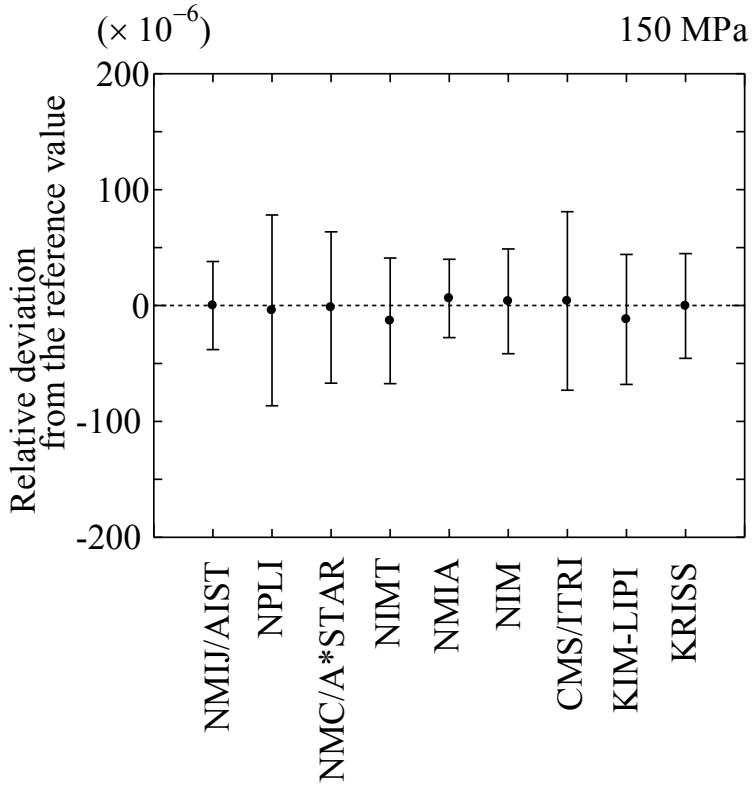
(× 10−6)
150 MPa
Relative deviation from the reference value
200
100
0
-100
-200
NMIJ/AIST
NPLI
NMC/A*STAR
NIMT
NMIA
NIM
CMS/ITRI
KIM-LIPI
KRISS

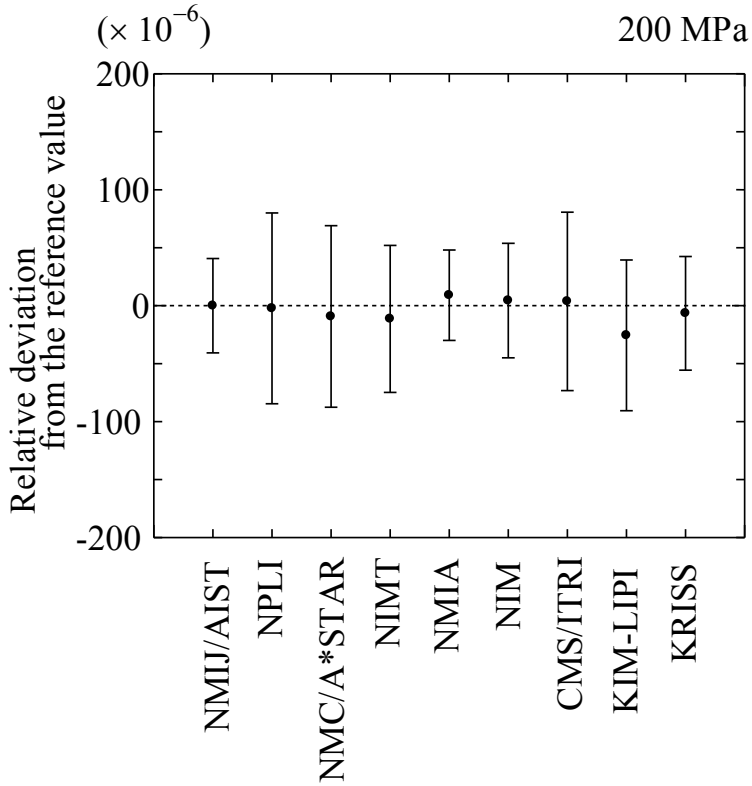
(× 10−6)
200 MPa
Relative deviation from the reference value
200
100
0
-100
-200
NMIJ/AIST
NPLI
NMC/A*STAR
NIMT
NMIA
NIM
CMS/ITRI
KIM-LIPI
KRISS

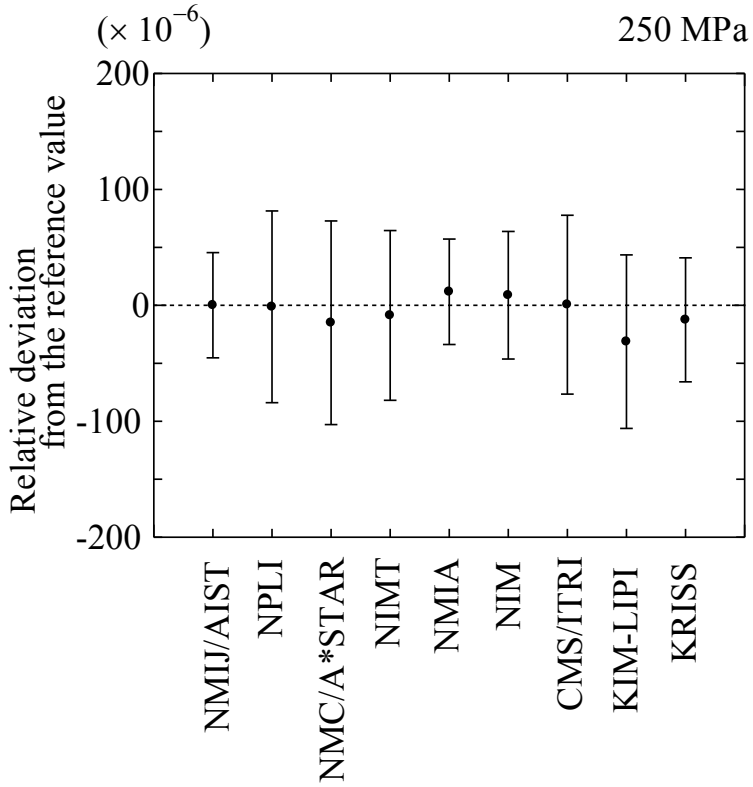
(× 10−6)
250 MPa
Relative deviation from the reference value
200
100
0
-100
-200
NMIJ/AIST
NPLI
NMC/A*STAR
NIMT
NMIA
NIM
CMS/ITRI
KIM-LIPI
KRISS

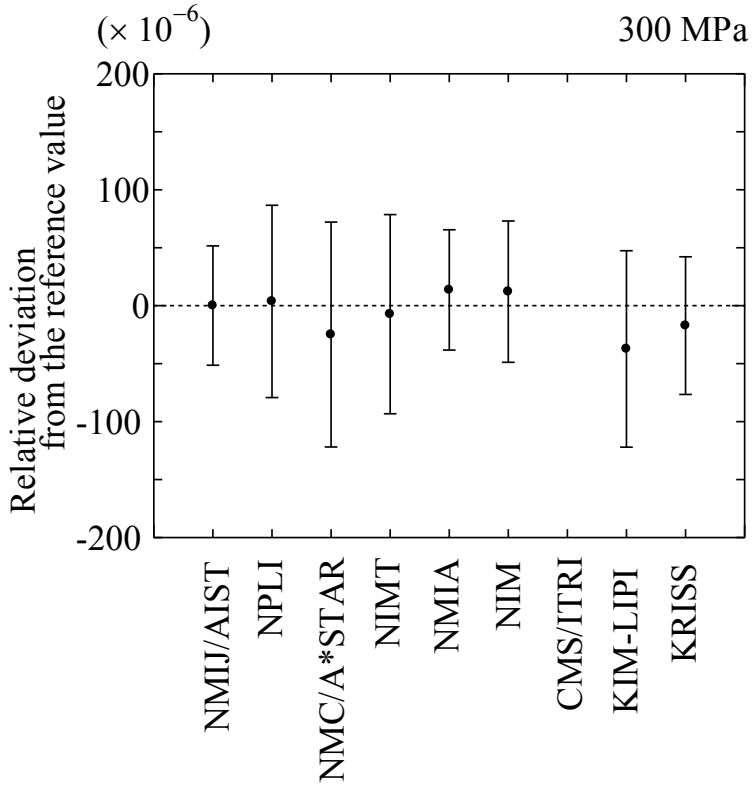
(× 10−6)
300 MPa
Relative deviation from the reference value
200
100
0
-100
-200
NMIJ/AIST
NPLI
NMC/A*STAR
NIMT
NMIA
NIM
CMS/ITRI
KIM-LIPI
KRISS

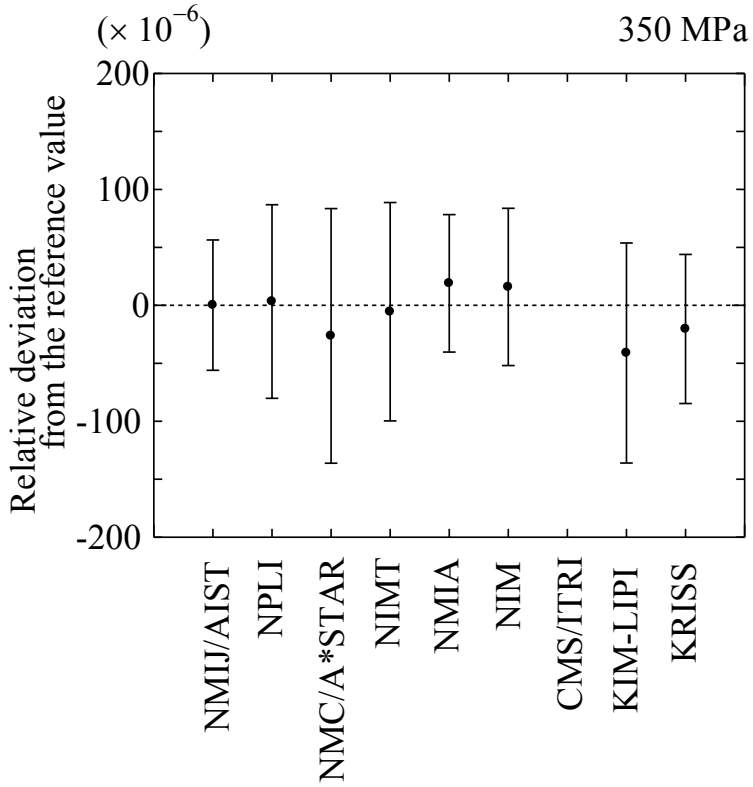
(× 10−6)
350 MPa
Relative deviation from the reference value
200
100
0
-100
-200
NMIJ/AIST
NPLI
NMC/A*STAR
NIMT
NMIA
NIM
CMS/ITRI
KIM-LIPI
KRISS

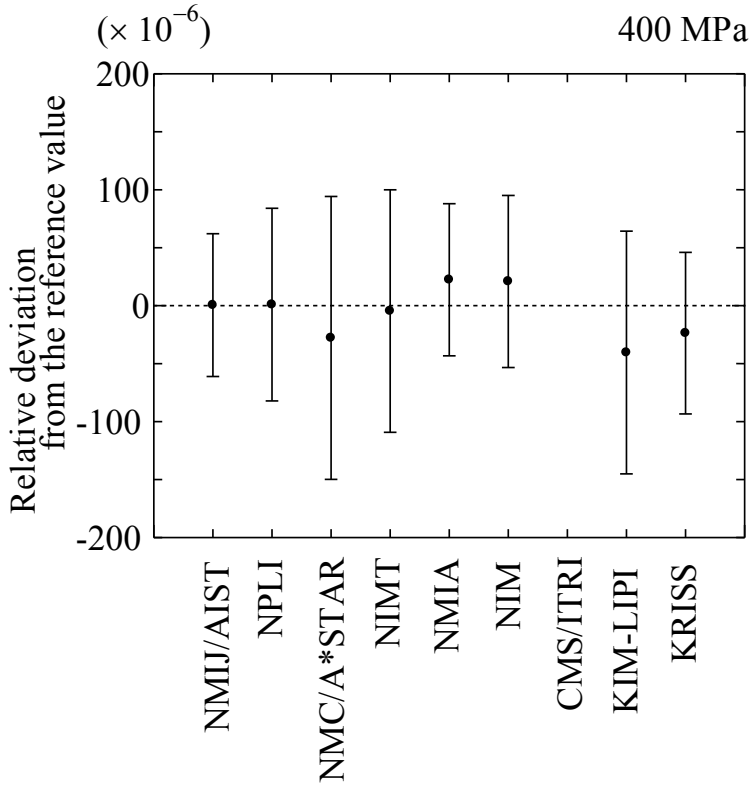
(× 10−6)
400 MPa
Relative deviation from the reference value
200
100
0
-100
-200
NMIJ/AIST
NPLI
NMC/A*STAR
NIMT
NMIA
NIM
CMS/ITRI
KIM-LIPI
KRISS

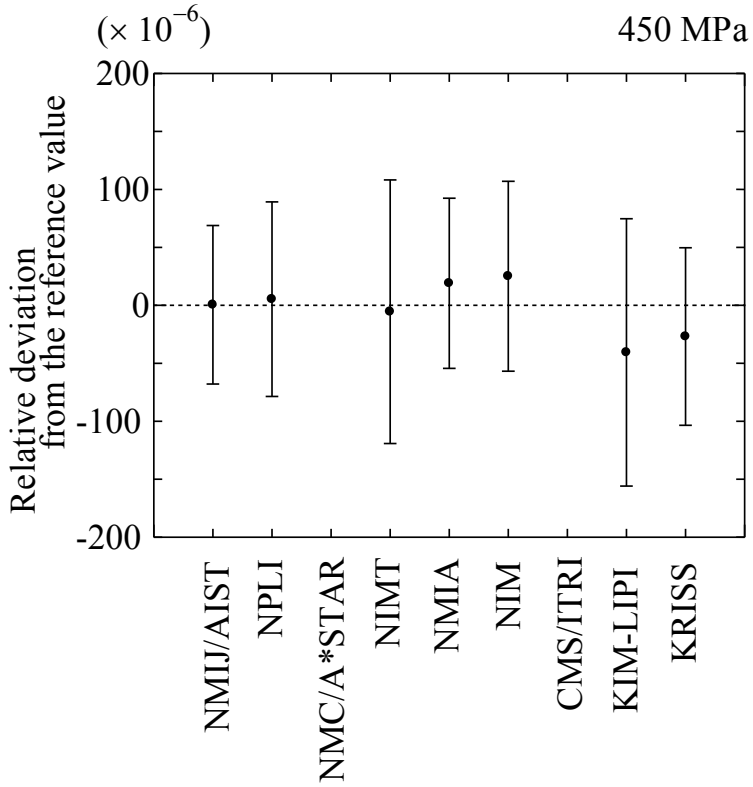
(× 10−6)
450 MPa
Relative deviation from the reference value
200
100
0
-100
-200
NMIJ/AIST
NPLI
NMC/A*STAR
NIMT
NMIA
NIM
CMS/ITRI
KIM-LIPI
KRISS

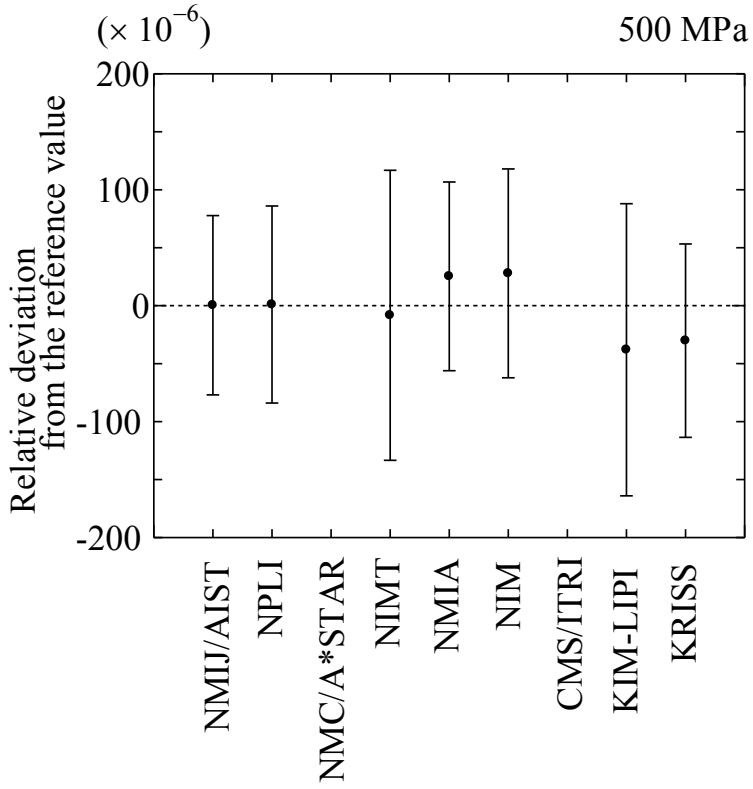
(× 10−6)
500 MPa
Relative deviation from the reference value
200
100
0
-100
-200
NMIJ/AIST
NPLI
NMC/A*STAR
NIMT
NMIA
NIM
CMS/ITRI
KIM-LIPI
KRISS